Bridging the gap between atomic scale and thermodynamics for structurally complex multiphase multi-element systems: metallic borides in Al-based metal-matrix composites as a case study

Rémy Besson, Ludovic Thuinet

Bridging the gap between atomic scale and thermodynamics for structurally complex multiphase multi-element systems: metallic borides in Al-based metal-matrix composites as a case study

R. Besson*, L. Thuinet

Univ. Lille, CNRS, INRAE, Centrale Lille, UMR 8207 - UMET - Unité Matériaux et Transformations, F-59000 Lille, France

Abstract

Intense researches on new kinds of materials, especially those with marked multi-principal-element character, currently give rise to all-intricate multiphase environments, for which reliably predicting structure and stability becomes extremely difficult to achieve with macroscopic phenomenological modellings. The purpose of this work is to demonstrate how this issue can be overcome by sticking down to the atomic scale, through ab initio-based thermodynamics within the Independent-Point-Defect Approximation (IPDA), which offers an efficient framework to investigate systems involving various chemistries and crystallographies. As a case study of significant intricacy, we consider ternary Al-B-Ti viewed as an approximant for Al-based alloys reinforced with TiB_2 particles and including AlB_2 and Al_3Ti additional compounds. Firstly, our IPDA investigations reveal unexpected discrepancies among neighbouring metallic borides, and predict point defect structures at odds with earlier pictures commonly employed hitherto, which suggests that many complex compounds may suffer from inadequate phenomenological modellings. Furthermore, we show that far-reaching conclusions on phase stability can be drawn only if the scope of analysis is broadened up to encompass global multiphase IPDA-based thermodynamics, a task which constitutes the core and the methodological originality of this work. Our approach thus provides reliable arguments to interpret the occurrence of various kinds of poorly known compounds, as illustrated by the controversial behaviour of Al_3Ti and AlB_2 in TiB_2-reinforced Al-based composites. Finally, our work allows to conclude that the robust and handsome IPDA approach can be extended to highly intricate multiphase situations, e.g. to investigate other classes of multiphase multi-principal-element materials, which

*Corresponding author. Tel.: +33 (0) 3 20 33 62 25
Email address: Remy.Besson@univ-lille.fr (R. Besson)

due to the presence of complex crystal structures can hardly be explored by alternative methods.

Keywords: point defects, ab initio calculations, thermodynamics, complex systems, metallic borides, aluminium alloys

1. Introduction

Unraveling the physical factors responsible for alloy stability still currently remains a hard challenge for most multicomponent and multiphase alloys elaborated in practice [1]. Quite often, the predictions for such inhomogeneous systems are crippled by the occurrence of a wealth of poorly-known phases, either intermetallic or involving light non-metallic elements (hydrides, borides, carbides, nitrides, oxides...), with complex crystal structures and chemistries, showing intricate long-range order and various critical stoichiometries associated with drastic changes of properties. Thus, it is indeed a common feature, in practical elaboration processes of alloys, to be faced with unexpected and ill-identified extra phases, which strongly complicates the interpretation of measurements and tuning of properties, a situation also encountered recently in multi-principal-element systems [2].

In principle, the answers to these questions should be provided by the knowledge of the thermodynamic properties of the various phases at stake, but the relevant experimental measurements may be extremely uneasy to carry out, and atomic-scale models and simulations thus offer an efficient alternative framework to deal with complex phases. While accurate ab initio methods can be employed to this aim, the issue here is twofold, since (i) it is a difficult task to build free energies from the atomic scale, and (ii) the upscaling towards more global macroscopic properties of complex alloys (e.g. multiphase equilibria), usually carried out on phenomenological grounds, may not be adequate, as illustrated below for aluminium alloys. Therefore, tractable and fully self-contained atomic-scale approaches sufficiently robust to open routes towards higher-scale properties in structurally complex multiphase systems are desirable, but they nevertheless remain too scarce in the current state of the art. To depict this situation more precisely, it is instructive to note that, in contrast with the extensive literature concerned with atomic-scale investigations of binary cubic systems (much more seldom higher-order [3] or lower-symmetry [4] ones) restricted to a single coherent lattice, atomic-scale explorations of multiphase stability have hardly addressed important families of materials such as Al-based alloys or steels [5, 6]. As emphasized above, these defi-

ciencies are due to the occurrence, in these widespread classes of materials, of many additional ordered phases with complex low-symmetry structures, which hardly lend themselves to modelling in widespread approaches such as cluster expansions, whereas these approaches can be employed successfully for high-symmetry and coherent systems recently including single-phase bcc- or fcc-based multi-principal-element alloys [7].

The present work aims at contributing to remedy these weaknesses, by proposing a comprehensive atomic-scale framework dedicated to yield reliable thermodynamic properties, noticeably definite and reliable chemical potentials, in various structurally complex multiphase alloy environments. To this purpose, considering the critical role played by phases involving some kind of long-range order, the underlying point defect structures provide the most relevant and physically safe background, and it is thus logical to explore the above issues from ab initio point defect-based thermodynamics of ordered compounds. This task can be best carried out via the so-called Independent-Point-Defect Approximation (IPDA) [8]. Due to its robustness and "chemically local" character centered on stoichiometry (see further remarks below), the IPDA can be employed in many difficult situations, involving complex crystallographies, e.g. recently for the Al_4Cu_9 compound [9], or the $MgZn_2$ Laves phase [10]. While firstly used in the realm of intermetallics, this approach can also be applied to other kinds of systems, as shown previously (e.g. for carbides [11] or carbonates [12]) and in the present work concerned with metallic borides. It also proved to be a useful tool to help investigate the effect of additional elements in ordered compounds, as shown e.g. for metallic elements in $Cr_{23}C_6$ carbides [11]. Most importantly, the IPDA provides an appealing framework - maybe the only one - for step-by-step, physically sound design of atomic-scale thermodynamics for structurally complex multiphase and multi-element materials, because of the clear-cut separation between the foundations of the method, namely (i) the ab initio energetics of point defects, (ii) the IPDA hypothesis of energetic independence of these defects, and (iii) the various ingredients (elementary point defects, more complex ones, defect phonons...) that can be included, or not, in a given IPDA model. While this triplet of separate foundations does also exist, to some extent, in alternative routes such as cluster expansions, the much more handsome formulation of IPDA allows to identify easily which route among (i)-(iii) should be followed, in order to improve specifically the thermodynamic description of a given phase. As a second noticeable advantage inherent to IPDA, this approach allows easy compound-selective improvements for the overall thermodynamic modelling of multiphase systems, by focusing on a given phase, without

inducing unphysical perturbations on the properties of other phases also modelled with IPDA. This flexibility stems from the fact that, in contrast with cluster expansion models, encompassing large composition domains, the IPDA is a "chemically local" approach fundamentally built on a separate analysis of the elementary excitations (point defects) characterizing each ordered compound around its stoichiometry. Indeed, the present work on Al-B-Ti will provide strikingly constrasting situations in this regard, showing how IPDA allows to treat separately the AlB_2 and TiB_2 compounds with a safe treatment of their specific point defect properties, in contrast with e.g. a single cluster expansion modelling of both borides [13, 14] viewed as end-members of a $(Al,Ti)B_2$ system limited to Al-Ti substitutions but disregarding all other point defect properties. Last but not least, our main concern being to use atomic-scale thermodynamics to carry out predictions of phase stability in complex multiphase alloys, the chemical potentials of the various elements in the various phases appear as the central quantities required to reach this target with efficiency, since (i) they are well-known to control the phase stability by determining the conditions of equilibrium and phase compositions, (ii) they also control the stability of various microstructural defects (interfaces...) by settling the excess energies of these defects. It is then noteworthy that, contrary to other atomic-scale approaches, the IPDA offers a convenient frame to determine and handle chemical potentials in complex multiphase environments.

In order to investigate these issues in detail, an appealing case-study is provided by aluminium alloys reinforced by ceramics, the so-called « Metal Matrix Composites » (MMCs). In these alloys, various poorly-known ordered phases are found to play a prominent role, (i) TiB_2 metallic borides, (ii) "chemically neighbouring" compounds such as AlB_2 or Al_3Ti, more or less transiently formed during elaboration processes, (iii) more "exotic" $Mg(Zn,Cu)_2$ Laves phases observed in final alloys, induced by addition elements and showing complex crystal structures. The ill-understood stability of these various compounds is determined by the chemical potentials of the various elements, either intrinsic ones or additions, present in the alloy. Moreover, since the properties of these alloys are determined by the interfaces between the Al-based main phase and TiB_2 or $Mg(Zn,Cu)_2$ particles [15, 16, 17, 18, 19], the direct dependence of interface energies upon chemical potentials implies that reaching a reliable knowledge of the overall stability of the multiphase system is of the utmost importance. Furthermore, Al-based MMCs offer a good example to illustrate our first remarks in this introduction on the intricacy of understanding phase stability and the limits of current predictive approaches. Noticeably, the various kinds of elaboration processes of TiB_2-reinforced Al-based

MMCs show transient appearance of additional phases, in particular Al_3Ti and AlB_2, which cannot be well justified from available knowledge.

To elucidate the role of these various phases in the elaboration processes of Al-based MMCs, previous works have been dedicated to the thermodynamic assessment of the Ti–B system using the Calphad methodology. In the framework of the compound energy formalism, the two-sublattice model $[(B,Ti\%)_1:(B\%,Ti)_2]$ was first used in [20, 21] to describe the TiB_2 phase, where the symbol % designates the major component in the related sublattice. This approach was then generalized in [22] to treat both diborides AlB_2 and TiB_2 in the ternary Al-B-Ti system by means of the following sublattice model $[(Al,B,Ti)_1:(B\%,Ti)_2]$. In such descriptions, it should be noticed that arbitrary assumptions are implicitly made concerning the nature of point defects occurring in these compounds, namely only antisites TiB or BTi and Al substitution in the sublattice associated to the metallic element. Quite surprisingly, other types of defects, like vacancies, were not considered. In this still ambiguous context, a goal of this work is then to revisit the models selected for metallic diborides, since these models are essential ingredient for a successful description of the phase diagram, using for example the optimization tool PARROT of the Thermo-Calc software [23]. Consequently, significant ambiguities also arise when considering AlB_2, which like its isomorphic TiB_2 counterpart, is eventually predicted as a roughly perfect line-compound in phenomenological thermodynamic calculations, whereas severe composition changes are suggested by recent atomic-scale investigations [13, 14]. These discrepancies may question the validity of stability predictions in multiphase contexts involving AlB_2, such as Al-based MMCs. This justifies the present fully atomic-scale investigations of multiphase stability in Al-B-Ti. As shown below, our major goal will be to demonstrate how IPDA thermodynamics offers a comprehensive way to unravel these issues, with atomic-scale sound physical grounds.

To answer these questions, the present work will consist of the following steps:

(i) Starting from elementary statistical physics, atomic-scale IPDA thermodynamics will be recalled for ordered compounds - to this aim, focus will be put on those compounds relevant in the context of Al-based alloys, but this is a pure matter of convenience and by no means restrictive;

(ii) A thorough IPDA analysis will be carried out for TiB_2(Al) titanium boride including Al additions;

(iii) A similar study on the neighbouring AlB_2 compound will point out surprising differences between both isomorphic borides, however detectable only if phase equilibria are included in the

analysis;

(iv) Confronting these metallic borides with the Al(B,Ti) solid solution, will then make it possible to predict larger-scale alloy properties embodied in isothermal sections of the Al-B-Ti phase diagram;

(v) Making connections with practical aluminium alloys, we will show how IPDA-based atomic-scale thermodynamics allows to interpret ill-understood behaviours and help to remove experimental controversies on phase stability in Al-based MMCs.

2. Methods

2.1. Ab initio calculations

All ab initio energy calculations in this work were performed with the VASP software [24], using the Projector Augmented Wave mode [25] and the GGA approximation with the PBE functional [26, 27]. The valence electrons for the pseudopotentials were $3s^2 3p^1$ (Al), $2s^2 2p^1$ (B) and $3s^2 3p^6 3d^2 4s^2$ (Ti). The energy cutoff for plane wave expansions was chosen equal to 500 eV throughout, and all k-point meshes were Γ-centered with $18\times18\times18$, $16\times16\times16$ and $18\times18\times18$ for single unit cells in fcc Al, TiB_2 and AlB_2 respectively. Total energies were calculated via the tetrahedron method including Blöchl corrections [28]. A first-order Methfessel-Paxton [29] smearing scheme was used, with a smearing width of 0.2 eV. These settings of parameters ensured reasonable accuracy for all total energies (below 10^{-3} eV/atom). Magnetism being immaterial in Al-B-Ti, spin polarization was not taken into account. All energy minimizations included the optimization of atomic positions as well as supercell volumes and shapes, corresponding to crystals modelled under zero pressure.

Using the elemental free energies G_0 of pure Al, B, Ti in their reference states (chosen to be fcc-Al, α-B12 and α-Ti), the formation free energy per atom G_f of a given compound $Al_xB_yTi_{1-x-y}$ is defined generally from its total free energy per atom G_t as:

$$G_f(Al_xB_yTi_{1-x-y}) = G_t(Al_xB_yTi_{1-x-y}) - xG_0(\text{fcc-Al}) - yG_0(\alpha\text{-B12}) - (1-x-y)G_0(\alpha\text{-Ti}) \quad (1)$$

Though G_0 and G_t should include all kinds (configurational, phonons, electronic [30]) of contributions to the alloy and elemental microstates, the approach below will include only configurational terms. More explicitly, while G_f should be decomposed as $G_f = G_f^{conf} + G_f^{ph} + G_f^{elec}$, the G_f^{ph} and G_f^{elec} terms will be approximated to be zero, while G_f^{conf} will be conveniently obtained

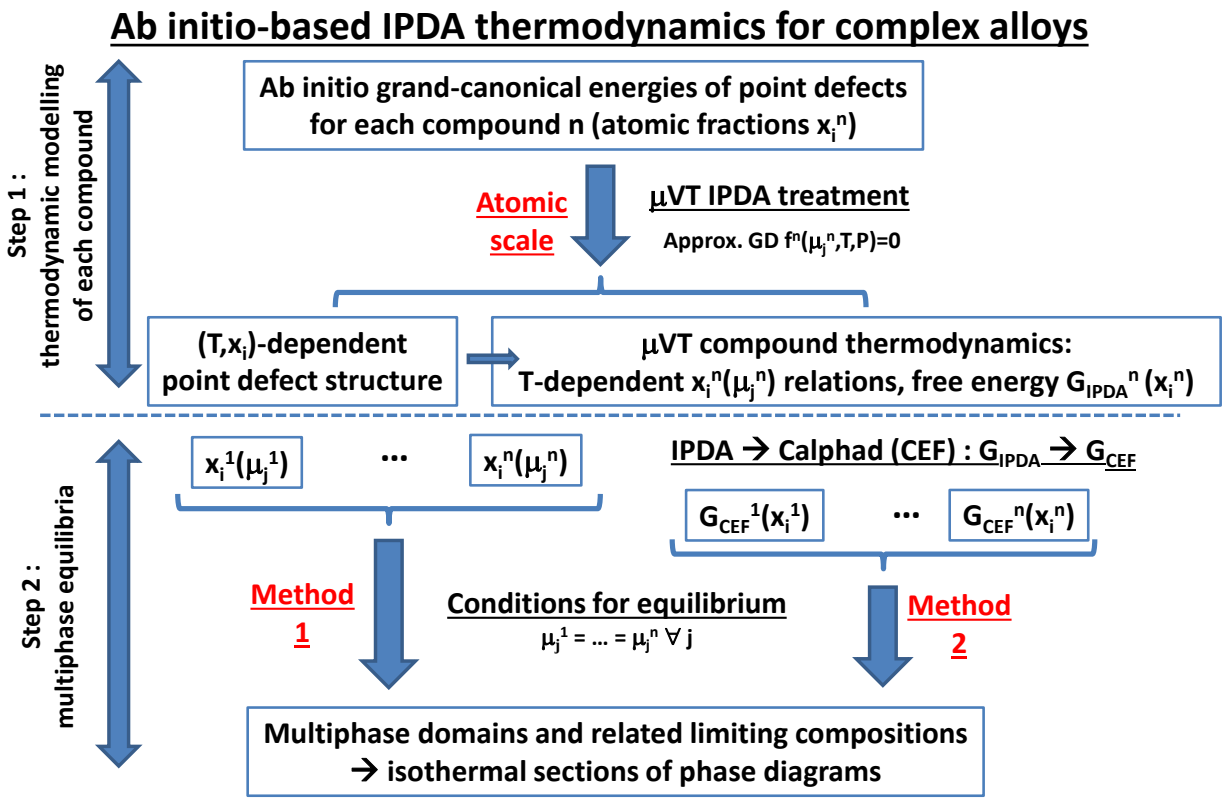

Fig. 1: Frame diagram of the DFT-based IPDA thermodynamics approach for multiphase equilibria. "Method 1" refers to a full derivation of phase equilibria within the IPDA context, as illustrated in the present work for Al-B-Ti; "Method 2" refers to a mixed scheme which corresponds to introducing the IPDA-derived free energies into the Calphad tools for phase equilibria, through a proper conversion via the Calphad Compound Energy Formalism (CEF) (see text for details).

from IPDA. Under this assumption, the reference free energies G_0 of eq. (1) can be identified to the ground-state energies E_0 derived from DFT, namely E_0(fcc-Al)=-3.748 eV/atom, $E_0(\alpha$-Ti)=-7.946 eV/atom and $E_0(\alpha$-B12)=-6.678 eV/atom.

Also required will be the total reference energies (per unit formula) of the perfect defect-free ordered compounds, namely $E_0(TiB_2)$=-24.476 eV, $E_0(AlB_2)$=-17.233 eV, and $E_0(Al_3Ti)$=-20.784 eV.

2.2. *Atomic-scale thermodynamics, low-symmetry phases and multiphase equilibria: the IPDA methodology*

As emphasized in the introduction, the IPDA modelling of ordered compounds [8] is a versatile and handsome approach to settle ab initio point-defect-based thermodynamics of multiphase materials with various types of ordered phases, either intermetallic ones or involving other kinds of elements (H, B, C, N, O...). For a binary ordered compound including a single addition element, the IPDA approach is now recalled briefly, using the most convenient μVT formalism. The starting point is the grand-canonical potential of each phase studied separately:

$$\Omega_{\mu VT} = E - TS - \mu_i N_i = -\frac{1}{\beta} \ln Z_{\mu VT} = -PV \tag{2}$$

($Z_{\mu VT}$ partition function, $\beta = \frac{1}{kT}$), which has to be minimized with respect to the amounts $\{N_d\}$ of point defects (PDs) of various kinds $\{d\}$, under proper constraints of matter conservation. Under the IPDA hypothesis, the $\{N_d\}$-dependent energy is, for a subsystem containing M unit cells:

$$E(v_0, M, \{N_d\}, \{V_d\}) \approx M e_0(v_0) + \sum_d N_d E_d^{GC}(v_0, V_d) \tag{3}$$

with:

$$E_d^{GC}(v_0, V_d) = E(V_d) - m_d e_0(v_0) \tag{4}$$

the so-called grand-canonical (GC) energy of PD of type d, and $E(V_d)$ the corresponding total energy, both defined for a volume V_d containing m_d unit cells around the defect, $e_0(v_0)$ being the energy of the perfect crystal per unit cell with volume v_0. A similar expression holds for the total volume:

$$V = M v_0 + \sum_d N_d V_d^{GC}(v_0, V_d) \tag{5}$$

with $V_d^{GC}(v_0, V_d) = V - m_d v_0$ the GC volumes.

Sublattices $\{r\}$ are essential ingredients of IPDA. For an A-B binary compound including A-type and B-type sublattices (in respective numbers R_A and R_B), together with supplementary interstitial sublattices, they are labelled as follows:

$$\begin{aligned}\rho_A &\equiv \{r \leq R_A\} \\ \rho_B &\equiv \{R_A < r \leq R_A + R_B\} \\ \rho_I &\equiv \{r > R_A + R_B\}\end{aligned} \tag{6}$$

In presence of an addition element C, and noting for convenience E_d^r the GC energy of PD of type d located on sublattice r, and V for vacancies, the energy becomes:

$$\begin{aligned}E = Me_0 &+ \sum_{r\in\rho_A}[N_B^r E_B^r + N_V^r E_V^r + N_C^r E_C^r] \\ &+ \sum_{r\in\rho_B}[N_A^r E_A^r + N_V^r E_V^r + N_C^r E_C^r] \\ &+ \sum_{r\in\rho_I}[N_A^r E_A^r + N_B^r E_B^r + N_C^r E_C^r]\end{aligned} \tag{7}$$

The PD-induced configuration entropy reads simply $S_c = -kMX$ with :

$$\begin{aligned}X = &\sum_{r\in\rho_A} p^r[x_B^r \ln x_B^r + x_V^r \ln x_V^r + x_C^r \ln x_C^r] \\ &+ \sum_{r\in\rho_B} p^r[x_A^r \ln x_A^r + x_V^r \ln x_V^r + x_C^r \ln x_C^r] \\ &+ \sum_{r\in\rho_I} p^r[x_A^r \ln x_A^r + x_B^r \ln x_B^r + x_C^r \ln x_C^r] \\ &+ \sum_{r=1}^{R} p^r z^r \ln z^r\end{aligned} \tag{8}$$

where:

$$\begin{aligned}z^r &= 1 - x_B^r - x_V^r - x_C^r \quad (r \in \rho_A) \\ z^r &= 1 - x_A^r - x_V^r - x_C^r \quad (r \in \rho_B) \\ z^r &= 1 - x_A^r - x_B^r - x_C^r \quad (r \in \rho_I)\end{aligned} \tag{9}$$

and p^r the number of sites of type r per unit cell, the various x quantities being the fractional amounts of PDs, measured with respect to the number of sites of the corresponding sublattice. It is

then convenient to define:

$$\begin{aligned}
&\alpha^r_{V\delta} = \exp\left[-\beta(H^r_V + \mu_\delta)\right] \\
&(r \in \rho_A, \rho_B) \\
&\alpha^r_{BA} = \exp\left[-\beta(H^r_B + \mu_A - \mu_B)\right] \\
&\alpha^r_{CA} = \exp\left[-\beta(H^r_C + \mu_A - \mu_C)\right] \\
&(r \in \rho_A) \\
&\alpha^r_{AB} = \exp\left[-\beta(H^r_A + \mu_B - \mu_A)\right] \\
&\alpha^r_{CB} = \exp\left[-\beta(H^r_C + \mu_B - \mu_C)\right] \\
&(r \in \rho_B) \\
&\alpha^r_{A} = \exp\left[-\beta(H^r_A - \mu_A\right] \\
&\alpha^r_{B} = \exp\left[-\beta(H^r_B - \mu_B)\right] \\
&\alpha^r_{C} = \exp\left[-\beta(H^r_C - \mu_C)\right] \\
&(r \in \rho_I)
\end{aligned} \tag{10}$$

involving the GC enthalpies $H^r_d = E^r_d + PV^r_d$ of PDs, their chemical potential-dependent formation enthalpies (factors of β), and:

$$\begin{aligned}
Y^r_A &= 1 + \alpha^r_{BA} + \alpha^r_{VA} + \alpha^r_{CA} \\
Y^r_B &= 1 + \alpha^r_{AB} + \alpha^r_{VB} + \alpha^r_{CB} \\
Y^r_I &= 1 + \alpha^r_{A} + \alpha^r_{B} + \alpha^r_{C}
\end{aligned} \tag{11}$$

with $\delta = A$ for $r \in \rho_A$, $\delta = B$ for $r \in \rho_B$. The fractional amounts of PDs are then simply:

$$\begin{aligned}
&x^r_B = \alpha^r_{BA}/Y^r_A \quad x^r_V = \alpha^r_{VA}/Y^r_A \quad x^r_C = \alpha^r_{CA}/Y^r_A \quad r \in \rho_A \\
&x^r_A = \alpha^r_{AB}/Y^r_B \quad x^r_V = \alpha^r_{VB}/Y^r_B \quad x^r_C = \alpha^r_{CB}/Y^r_B \quad r \in \rho_B \\
&x^r_A = \alpha^r_{A}/Y^r_I \quad\quad x^r_B = \alpha^r_{B}/Y^r_I \quad\quad x^r_C = \alpha^r_{C}/Y^r_I \quad\quad r \in \rho_I
\end{aligned} \tag{12}$$

from which the atomic fractions in the compound can be derived straightforwardly.

This formalism will be applied below for both metallic borides with additions, namely TiB_2(Al) and AlB_2(Ti). Moreover, being easily transposable to a disordered system containing a single intrinsic element and an arbitrary number of additions, it will also be employed to study the Al(B,Ti) solid solution of B and Ti in fcc aluminium, thus ensuring that all phases are treated in a fully consistent way.

As a remarkable advantage, the μVT framework for IPDA provides the PD structure and derived thermodynamic properties in a relatively straightforward way. This convenience, related to the role

of chemical potentials as control variables, however relies widely on the use of an approximate Gibbs-Duhem (GD) relation $\sum_i x_i^0 \mu_i = E_0$ for each ordered phase investigated, where the sum extends on the intrinsic species of the phase only (not on additions), while x_i^0 are the atomic fractions of these (intrinsic) species in the perfect defect-free compound of constant energy E_0. In the present work, all phases are thus treated in IPDA with approximate GD relations, namely:

- GD(TiB_2): $\mu_{Ti} + 2\mu_B = E_0(TiB_2)$ for TiB_2(Al);
- GD(AlB_2): $\mu_{Al} + 2\mu_B = E_0(AlB_2)$ for AlB_2(Ti);
- GD(Al): $\mu_{Al} = E_0$(fcc-Al) for the fcc Al(B,Ti) solid solution.

As regards the Al_3Ti compound, also close to the Al+TiB_2 domain, its IPDA modelling and role in multiphase equilibria were left for future work. It can be recalled that the exact form of GD relations should involve compound free energies (thus including off-stoichiometry-dependent configurational entropies). However, this issue is not critical: though slightly more cumbersome, including exact GD relations in the IPDA framework is easily achievable (and was added as an option in the IPDA toolbox), and tests performed on the Al-B-Ti phases of interest have indicated that this refinement in modelling can be safely neglected in the present case. More generally than Al-B-Ti, the validity of approximate GD relations in the context of IPDA can be easily understood, as IPDA corresponds to moderate off-stoichiometries and amounts of point defects, hence a limited effect of off-stoichiometry-dependent terms in compound entropies.

Anticipating on a more detailed and quantitative analysis of thermodynamic equilibria in Al-B-Ti (section 3.4 below), it is interesting to make a connection, through the B and Ti chemical potentials in TiB_2, between the above IPDA model for TiB_2 and the occurrence of the Al+TiB_2 two-phase domain characteristic of Al alloys reinforced by TiB_2. This domain is bounded on either side by a couple of three-phase systems, either Al+TiB_2+Al_3Ti or Al+TiB_2+AlB_2, each corresponding to limiting values of the B or Ti chemical potentials. These limiting values, often required to discuss interface stability in systems such as Al+TiB_2 [15, 16, 31, 19] (see remarks in Introduction above, and Appendix B of Ref. [19] for a clear determination of these values), are usually assessed in a simplified way, under the assumption of perfect PD-free stoichiometric compounds TiB_2, AlB_2 and Al_3Ti, the Al(B,Ti) solid solution being assimilated to pure fcc Al, namely using the approximate GD relations introduced previously. Under these hypotheses, the range of chemical potentials expressed in terms of μ_{Ti}, associated with the stability domain of the two-phase Al+TiB_2 system, is:

$$\mu_{Ti}^{\text{inf}} \leq \mu_{Ti} \leq \mu_{Ti}^{\text{sup}} \tag{13}$$

with μ_{Ti}^{inf} =-10.989 eV/atom and μ_{Ti}^{sup} =-9.540 eV/atom. In this paper, the same condition will be also expressed in terms of $\Delta\mu_{Ti} = \mu_{Ti} - E_0(\alpha\text{-Ti})$:

$$-3.043 \text{ eV/atom} \leq \Delta\mu_{Ti} \leq -1.594 \text{ eV/atom} \tag{14}$$

Combined with the above approximate GD relation for TiB_2, eq. (13) can be converted in terms of B chemical potential, leading to:

$$-7.469 \text{ eV/atom} \leq \mu_B \leq -6.746 \text{ eV/atom} \tag{15}$$

As shown below, the IPDA will allow to determine conveniently the features of the two-phase Al+TiB_2 domain, notably the tie-lines. To this aim, the following procedure will be adopted, based on the usual equality of chemical potentials between phases at equilibrium:

* the GD(Al) relation for the Al-based phase sets the Al chemical potential in both phases:

$$\mu_{Al}^{\text{TiB}_2} = \mu_{Al}^{\text{fcc-Al}} = E_0(\text{fcc-Al}) \tag{16}$$

* each tie-line corresponds to a given value of e.g. the B chemical potential in both phases, from which the Ti chemical potential can be deduced by means of the GD(TiB_2) relation ;

* this set of $(\mu_{Ti}, \mu_B, \mu_{Al})$ yields the equilibrium compositions of the two phases ;

* a scanning of μ_{Ti} in the interval of eq. (13) provides the full tie-line structure.

The frame diagram of the proposed approach is displayed on Fig. 1.

3. Results

3.1. Preliminary: IPDA for Al(B,Ti) solid solution

Although IPDA is mostly relevant for ordered compounds involving two or more intrinsic elements, it can also be used for solid solutions built on a single base element. In order to investigate phase equilibria in Al-based alloys, a preliminary step is required, consisting in IPDA modelling of the Al(B,Ti) solid solution. The total energies of the point defects selected for Al(B,Ti) are listed in Supplemental Material, all species being allowed to occupy both kinds (O and T) of interstitial sublattices. Considering supercells of various sizes, the corresponding GC energies (see figure in

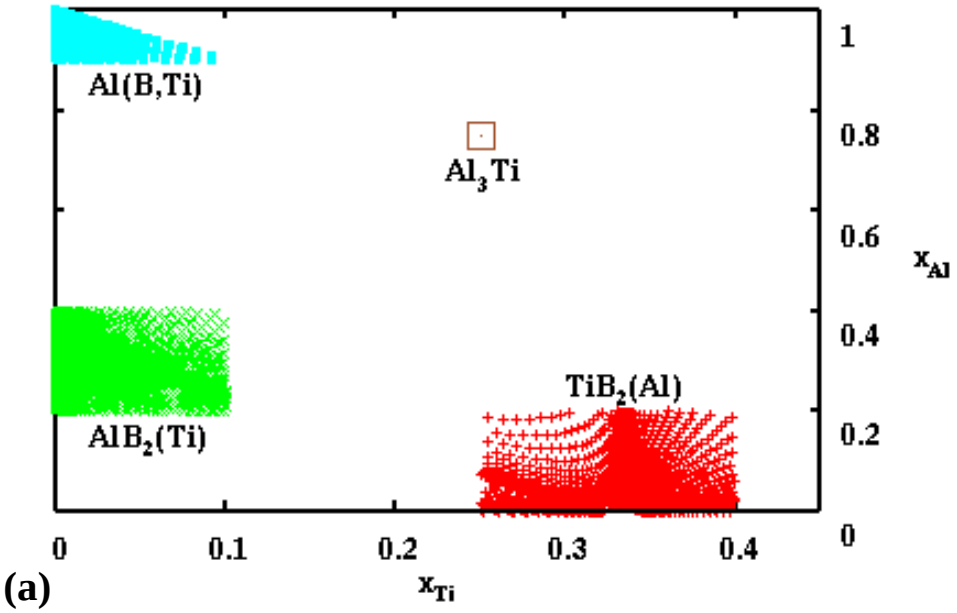

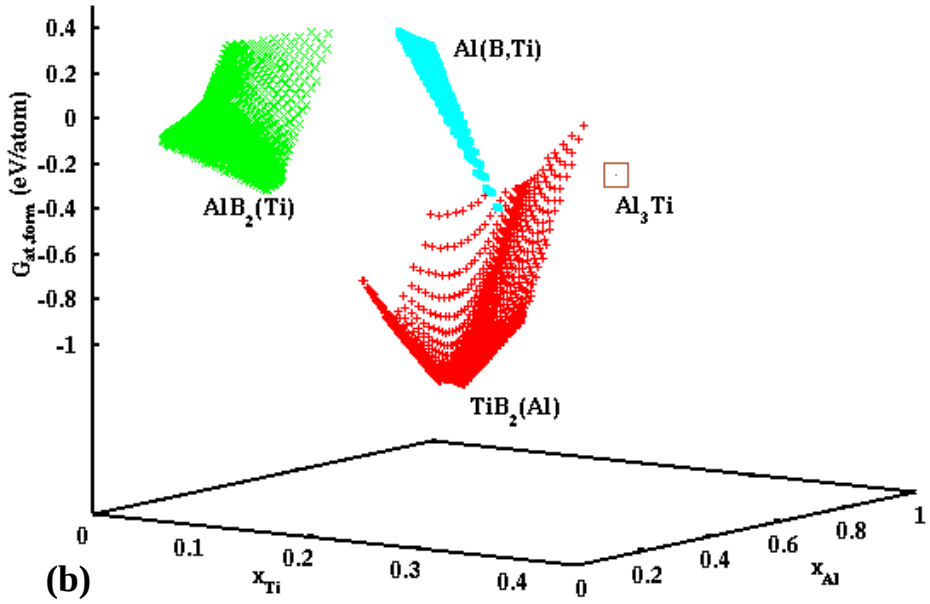

Fig. 2: Using IPDA-based thermodynamics, free energy surfaces at 1000 K and zero pressure for the Al(B,Ti), TiB_2(Al) and AlB_2(Ti) phases studied in this work: (a) top view showing the composition domains explored in the (x_{Ti},x_{Al}) plane ; (b) 3D overview of formation free energies. The energy of perfect point defect-free Al_3Ti is also displayed, since this compound, while not studied from IPDA in this work, was however used similarly to AlB_2, to delimit the two-phase Al(B,Ti)+TiB_2(Al) domain on the phase diagram (see below in text).

Supplemental Material) show reasonable convergence for 4x4x4 supercells. The latter values were thus used to obtain the resulting point defect properties of Al(B,Ti) at 1000 K (see Supplemental Material). This task was carried out under the approximate GD(Al) relation $\mu_{Al} = E_0(\mathrm{Al})$ (cf. previous section), which will be used recurrently in this work, as it provides the most convenient starting point to settle IPDA phase equilibria between Al(B,Ti) and the borides investigated below. In the present case of Al(B,Ti) modelling, which overlooks all complex defects coupling the chemical species, point defects involving Ti and B are respectively functions of the Ti and B amounts in the solid solution. As expected, Ti preferentially substitutes for Al, while B mainly occupies octahedral interstitial sites. As regards Al defects, under the same approximation, their amount is simply independent of the composition of the solid solution, with a marked preference for Al vacancies, interstitial occcupancy being negligible for this element, as expected. The point defect properties of Al(B,Ti) derived from IPDA then provide direct access to the free energy of this phase (Fig. 2, blue color), selecting 1000 K as a temperature representative of the experimental conditions encountered in alloy elaboration and use. As shown on Fig. 2(a), the composition domain explored covers a few at. % of Ti and B, a range consistent with the IPDA hypothesis and sufficient for our purpose. On the whole, this IPDA modelling of the Al(B,Ti) solid solution provides a reasonably sound picture, allowing to investigate below more intricate situations implying equilibria with ordered compounds.

3.2. IPDA study of TiB_2(Al)

TiB_2 is probably the most important ordered compound for Al-based MMCs, due to its presence as a dispersion of fine strengthening particles. This compound being a cornerstone of Al-based MMCs, it is therefore of the utmost importance to ensure that its thermodynamic modelling is reliable, before attempting to include it into multiphase contexts. IPDA is an efficient tool to perform this task, but surprisingly, the study of its point defect (PD) properties has not been carried out so far. For purpose of analyzing the equilibrium between TiB_2 and surrounding fcc Al-based solid solution, Al substitutional additions should also be included in the panel of PDs for TiB_2. As regards the presence of Al on the interstitial sites of the TiB_2 structure, this possibility cannot be discarderd a priori for simple reasons such as strong difference in atomic sizes. Therefore, preliminary tests, not reproduced here for brevity, were carried out, leading to conclude that such defects are indeed negligible in TiB_2(Al), as their concentration never exceeds vanishingly low values (10^{-50}) at 1000

K. Even when restricting to substitutional sites, the propensity of TiB_2 to accept Al as an additional element is not obvious, especially when TiB_2 is surrounded by (and in equilibrium with) an Al(B,Ti) solid solution. Getting a precise knowledge of these subtle features therefore constitutes a major target of this section. To this aim, the IPDA analysis was carried out for TiB_2(Al) under the approximate GD(TiB_2) relation (cf. section 2.2), thus supposed to be valid in presence of Al additions. The required IPDA input parameters, displayed as Supplemental Material, are the total energies of the various PDs relevant for TiB_2(Al), as a function of the supercell size used in ab initio calculations. The resulting GC energies (see also Supplemental Material) show reasonable convergence (within a few meV) with 5x5x5 supercells, the latter supercell size being therefore used throughout in the subsequent analysis of this compound.

3.2.1. Binary TiB_2

It is natural to start by considering TiB_2 as a reference four-PD compound, namely including only both types of antisites (Ti_B and B_{Ti}) and vacancies (V_B and V_{Ti}), the index referring to the sublattice bearing the PD. The resulting PD structure of this reference compound is displayed on Fig. 3 around stoichiometry at (a) 1000 K, this temperature being typical of elaboration processes, and (b) 3000 K close to the melting point of the compound. The main trend to be noted is probably the stepwise character of the PD concentration profiles, with either type of vacancy as dominant defect, antisites being formed in much lower quantities. Moreover, this character appears to be remarkably stable up to higher temperatures (Fig. 3(b)), which indicates a strongly ordered structure for TiB_2, even close to the solid$\rightarrow$ liquid phase transition. It also suggests that the temperature dependence of the PD properties of TiB_2 is well captured by the IPDA approximation. TiB_2 thus clearly appears as a vacancy-type ordered compound at all temperatures of interest. Fig. 3 also displays the approximate IPDA trends for TiB_2, as derived from straightforward simplified analytical expressions (given in Supplemental Material). This analytical approach was pointed out previously [32] as valuable for off-stoichiometric ordered compounds in which the structural PDs remain dominant when the temperature increases, which is indeed the case for Ti and B vacancies in TiB_2 on either side of stoichiometry. As a consequence of this clear-cut PD behaviour of TiB_2, the numerical and analytical predictions of IPDA are found in excellent agreement in this compound, which thus appears as a highly favourable case for IPDA thermodynamic modelling.

Before proceeding further towards multiphase stability in Al-based alloys, the possibility of in-

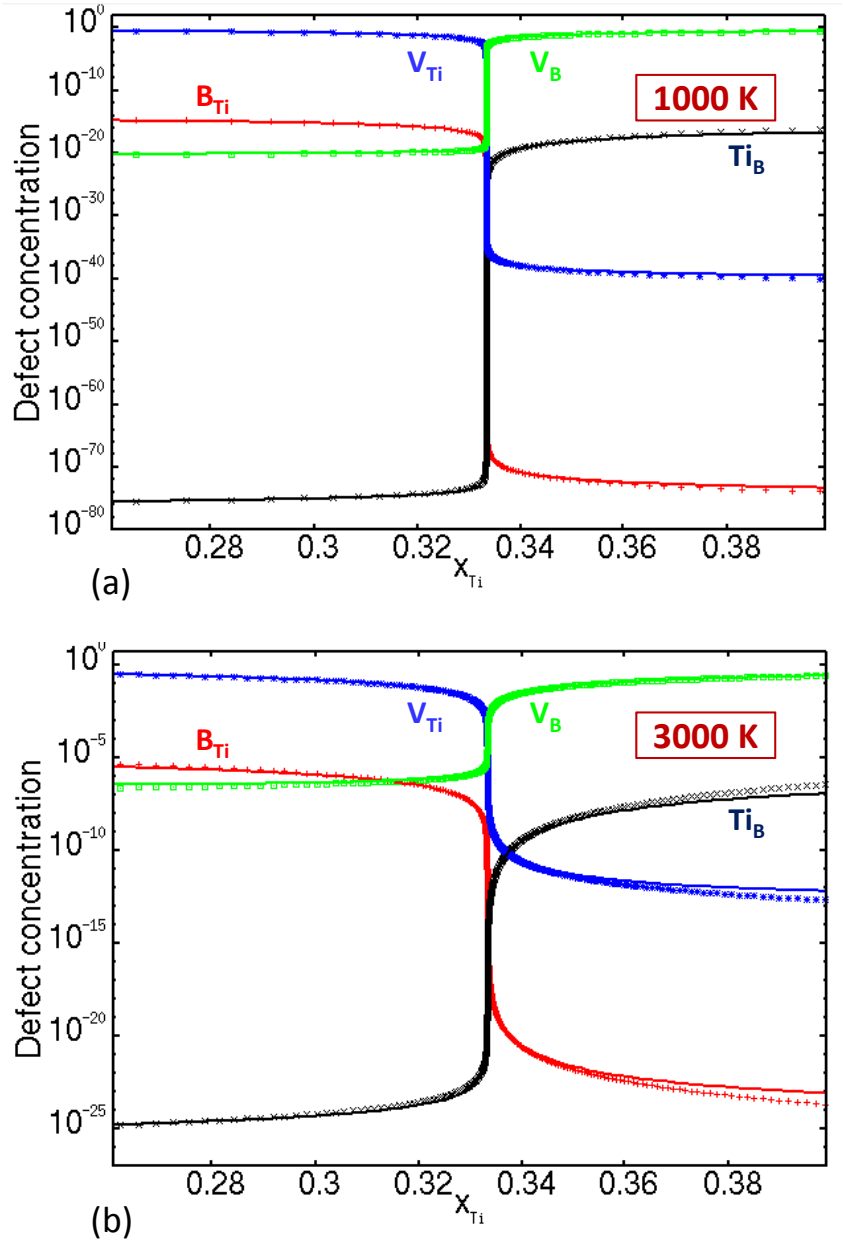

Fig. 3: Concentrations (cf. equations (12)) of intrinsic point defects (vacancies and antisites) in TiB_2 around stoichiometry, from ab initio-based IPDA thermodynamics: (a) 1000 K (typical of elaboration processes of Al alloys), (b) 3000 K (approaching the TiB_2 melting point). Point symbols and lines respectively denote the exact numerical-IPDA calculations and their analytical-IPDA approximations.

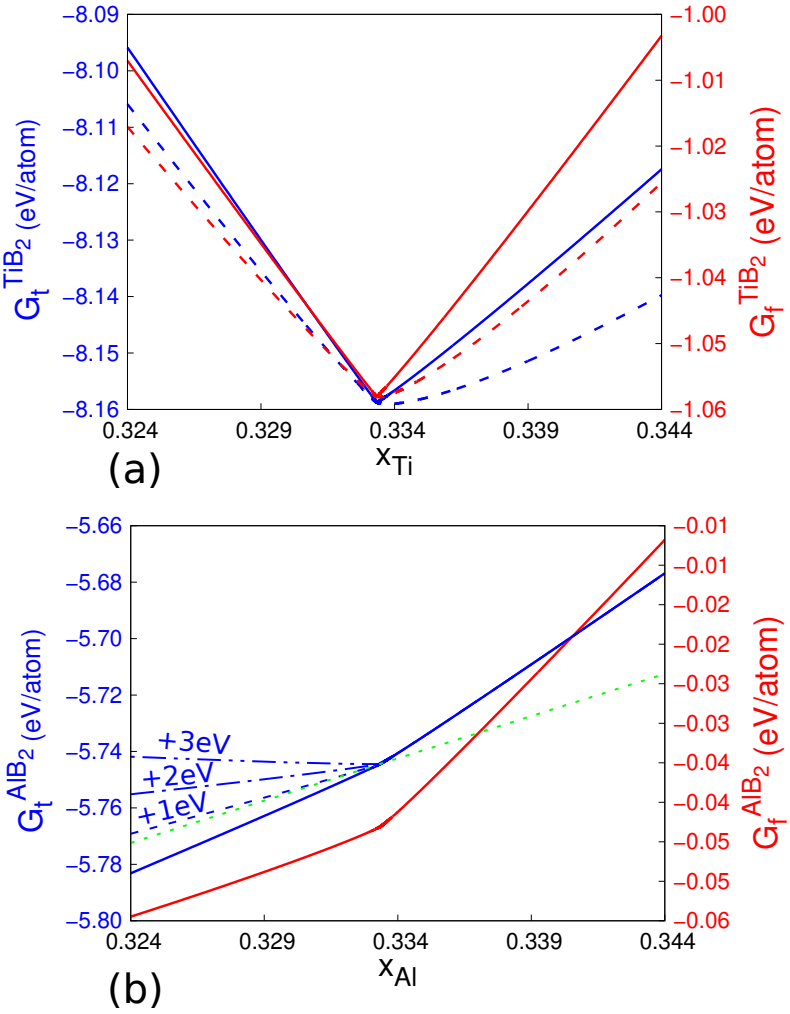

Fig. 4: (a) Total (blue) and formation (red) free energy of TiB_2, from ab initio-based IPDA thermodynamics, at 1000 K (full lines) and 3000 K (dashed lines), (b) same quantities at 1000 K for AlB_2. In (b), the effect of increasing the GC energy of the Al vacancy is also displayed (mixed blue lines), and the green dashed line depicts the GC energy increase threshold for which equilibrium between Al and the stoichiometric compound can be recovered (see text for details).

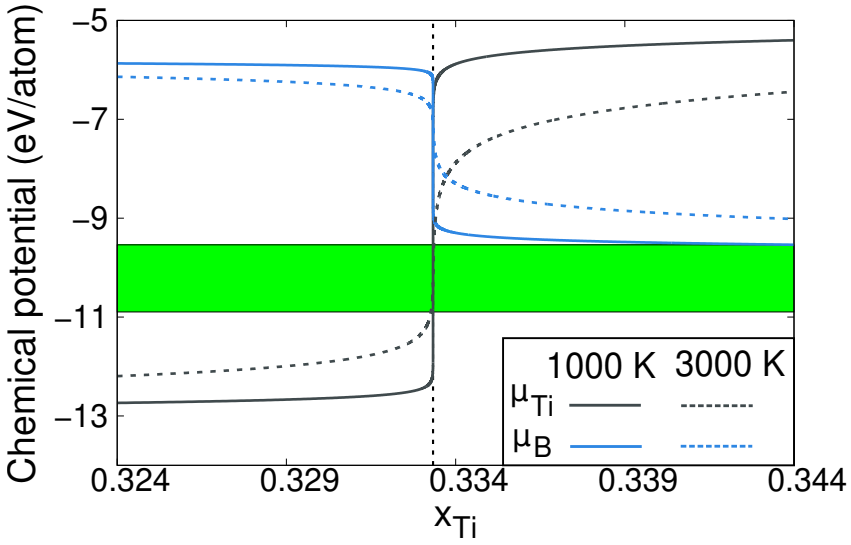

Fig. 5: Chemical potentials of B (blue) and Ti (black) in TiB_2 at 1000 K (full lines) and 3000 K (dashed lines), from ab initio-based IPDA thermodynamics. The green area indicates the range of Ti chemical potential for the (Al)+TiB_2 two-phase domain, while the lower and upper limits of this area correspond to the formation of a third phase, either AlB_2 or Al_3Ti respectively. From these IPDA curves, it can be concluded that the Ti composition of TiB_2 compatible with the Ti chemical potential values included in the green area is very close to the stoichiometric one.

terstitial occupancy for B in TiB_2 should now be investigated. Indeed, some unexpected dramatic effect of interstitials in low-symmetry sites was evidenced quite recently in previous IPDA studies of ordered compounds, e.g. for C in $Cr_{23}C_6$ carbides [11]. In order to include interstitial PDs in the previous reference IPDA model for TiB_2, and considering Ti as well as B for the sake of completeness, the required total energies on various interstitial sites (1b;2c;3f;3g) were calculated for increasing supercell sizes, 5x5x5 supercells being found sufficient for reasonable convergence. The PD amounts derived at 1000 K (cf. Supplemental Material) clearly indicate that, contrary to intuitive expectations due to the low atomic radius of boron, interstitial PDs should have no influence in TiB_2 (concentrations below 10^{-20}), at least if complex PDs involving B are overlooked. Thus, the reference four-PD structure (Fig. 3), involving only vacancies and antisites as major and secondary PDs, remains valid.

On the whole, the above IPDA model for TiB_2 seems reasonable (no PDs overlooked), and can thus be used to investigate the related thermodynamic properties of this compound, primarily its total and formation free energies (Fig. 4(a)). The free energy profiles of TiB_2 have expected sharp V-like shapes, consistent with near-perfect stoichiometry, a trend that will be discussed further below, by confronting Ti and Al borides. For comparison, Fig. 4(a) also displays the free energy at 3000 K, showing that the effect of temperature is much more important in Ti-rich compounds. In the context of Al-based alloys, the interest of such profiles is however limited, since equilibria between TiB_2 and other B-Ti binary phases such as Ti(B) or B(Ti) solid solutions do not reflect the alloy properties, and Al should therefore be introduced. The green-shaded area on Fig. 5 delineates the range of chemical potentials, expressed in terms of μ_{Ti} by eq. 13, associated with the stability domain of the two-phase Al+TiB_2 system (section 2). The intersection of this area with the IPDA profiles demonstrates that TiB_2 should be almost perfectly stoichiometric in this domain. This conclusion will be discussed in detail below, as phase equilibria will be assessed quantitatively at 1000 K (phase boundaries in composition space), by taking into account the presence of Al as addition element in TiB_2, together with the B and Ti solubilities in Al.

3.2.2. Addition of Al in TiB_2

Following our guidelines towards multiphase equilibria in Al-based MMCs, the interactions of TiB_2 with Al additions must now be explored. To carry out this study of TiB_2(Al), the IPDA methodology remains applicable, relying on total energies of Al substitutional PDs (as explained above,

the possibility of interstitial Al was not considered further), with reasonable convergence of GC energies ensured for 5×5×5 supercells for Al substitutional PDs (cf. Supplemental Material).

In order to get a clear overview of the properties of TiB_2(Al), it is instructive to perform first a T = 0 K analysis of this ternary compound, by means of the constant-composition (NPT) framework of IPDA, which at 0 K reduces to a constrained linear problem of enthalpy minimization. Despite its limited interest in binary TiB_2, this analysis becomes more valuable when the picture on PDs becomes more difficult to grasp, for example at finite temperatures when the dimension of the composition space increases. The 0 K analysis offers the advantage of simplifying the description, by focusing on the so-called "structural" PDs which subsist at lower temperatures. The results of this 0 K analysis for TiB_2(Al) are displayed on Fig. 6, as function of the Ti and Al atomic fractions. Remarkably, a strong composition dependence is found, as Al may substitute either for Ti or B, respectively for $x_B > 2/3$ and $x_{Ti} > 1/3$. For increasing Al contents in the compound, this effect can be qualitatively seen as a filling of the available vacant sites associated to the dominant V_B or V_{Ti} defects. The presence of Al in TiB_2 also induces the emergence of two limiting composition lines for $x_B = 2/3$ and $x_{Ti}=1/3$, with abrupt changes of the PD structure if the Al content crosses these thresholds. Surprisingly, between these two limits, an intermediate composition domain is found, in which vacancies (the major defects in Al-free TiB_2) are ruled out, while Al addition is found to substitute both for B and Ti. While the role of vacancies in TiB_2 is currently not well known, it may be expected that their Al-induced expelling may have consequences on the properties of TiB_2 particles (e.g. atomic diffusion inside them) inserted into Al alloys, if these particles are constrained, by multiphase equilibria, to have compositions lying within the intermediate domain shown on Fig. 6. It may thus be important to check whether TiB_2(Al) particles in practical Al-based alloys should be expected to lie within this vacancy-free domain of composition, the complexity of this issue being probably enhanced further by the simultaneous competitive presence of other additions (Cu, Mg...) in these alloys. On this figure are also specified the T = 0 K values for the elemental chemical potentials, showing their strong variations when crossing the limiting lines, which can be seen as a 3D extension of the sharp profiles of Fig. 5. Noticeably, since the Al chemical potential in Al-based alloys is expected to be close to the energy of pure fcc Al (approximate GD(Al) relation μ_{Al} = -3.748 eV/atom, cf. previous section), its actual level around the $x_B = 2/3$ line may leave room for TiB_2 undergoing severe PD-dependent changes, through possible switches, determined by the precise multiphase equilibrium conditions of the alloy, between the $x_B > 2/3$ domain and the intermediate

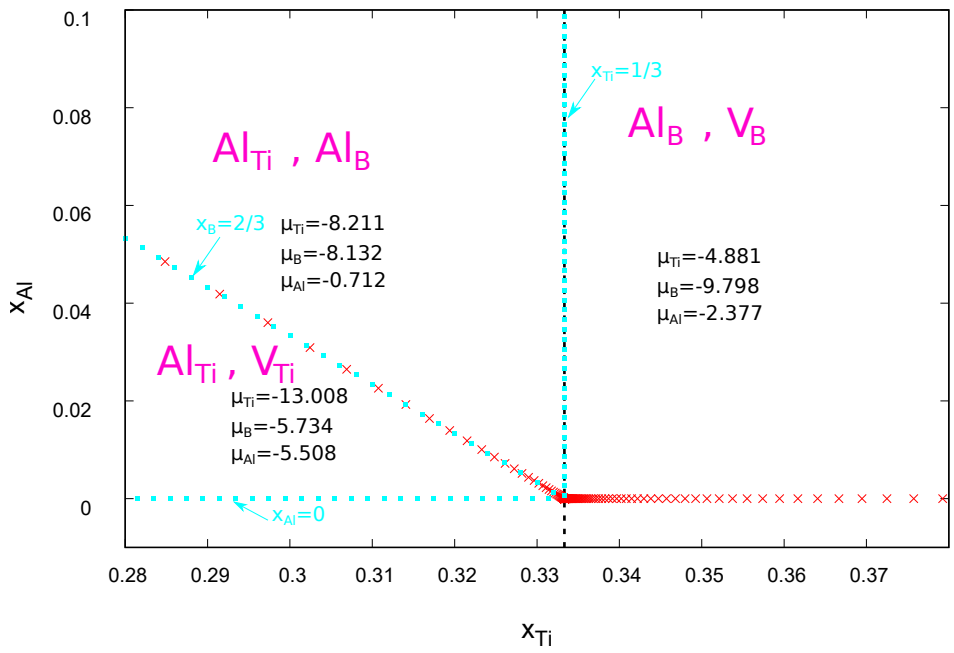

Fig. 6: IPDA thermodynamics for TiB_2 in presence of Al: overview of PD structure for the limiting case of T = 0 K. The structural PDs and elemental chemical potentials (eV) are indicated in each composition domain. The red cross symbols correspond to the path at constant Al chemical potential, with value equal to the energy of perfect pure fcc Al, i.e. μ_{Al} = E_0(Al) = -3.748 eV/atom characteristic of equilibrium with the fcc-based Al(B,Ti) solid solution (see further analysis at 1000 K).

vacancy-free one. Further details on this issue will be given below, by considering more thoroughly phase equilibria.

Our purpose being to investigate multiphase equilibria, a task that cannot be achieved realistically at 0 K [5], the effect of temperature must now be included in the IPDA model of TiB_2(Al), which leads to the 3D free energy surface at 1000 K as illustrated on Fig. 2 (red color). The corresponding 3D profiles for PD amounts, extending those of Fig. 3 and more difficult to handle, are not mandatory for further analysis. In the context of Al-based MMCs, it is much more relevant to investigate the TiB_2(Al) properties under the μ_{Al} = -3.748 eV constraint imposed by the approximate GD(Al) relation and Al+TiB_2 equilibrium, which corresponds to a path in the (x_{Ti},x_{Al}) plane

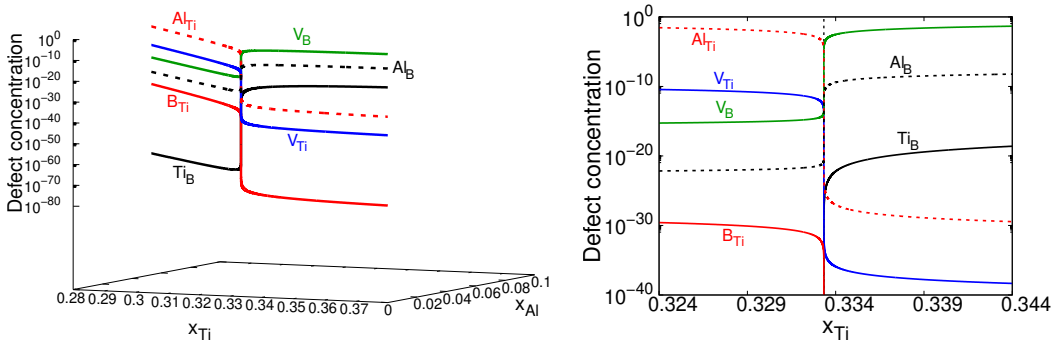

(a) (b)

Fig. 7: Concentrations of PDs in TiB_2(Al) in presence of Al at 1000 K, from IPDA thermodynamics, along the path of constant μ_{Al} = E_0(Al) = -3.748 eV/atom, characterizing equilibrium between Al and TiB_2: (a) 3D overview, (b) projection showing the x_{Ti} dependence. Full and dashed lines pertain to intrinsic and Al defects respectively.

(Fig. 7(a)). For easier reading, the results are recast into a more convenient form for analysis on Fig. 7(b), drawn solely as function of the Ti amount in the compound. Comparison with Al-free TiB_2 (Fig. 3) evidences strong Al-induced changes in PDs, in particular a drastic vanishing of Ti vacancies for $x_{Ti} < 1/3$, together with significant substitution of Al on Ti sites. This constant μ_{Al} path is also reported on Fig. 6 (red crosses), confirming that equilibrium with Al should indeed constrain TiB_2 into a domain of critically varying properties. From Fig. 6, the equilibrium μ_{Al} value lies approximately midway between the chemical potentials relative to the couple of neighbouring PD domains separated by the line x_B=2/3. It is interesting to note that this feature, responsible for the superposition of the equilibrium path (red crosses) and the line separating these domains (blue dots), should be highly specific to Al+TiB_2. It also shows the limits of the previous 0 K analysis to characterize the PDs of TiB_2(Al) in this two-phase system: this analysis allows to conclude reliably that Al should substitute for Ti rather than B (a property that could be questioned for higher values of μ_{Al}, closer to the -2.377 eV level on Fig. 6 and possibly encountered in environments implying e.g. liquid Al), but provides no information on the secondary PDs (Al_B or V_{Ti}?) around x_B = 2/3. On the whole, our analysis strikingly illustrates the fact that the properties of TiB_2 particles in Al-based alloys should be highly dependent on their surrounding.

As introduced previously for binary TiB_2 (Fig. 5), the current IPDA analysis of TiB_2(Al) easily

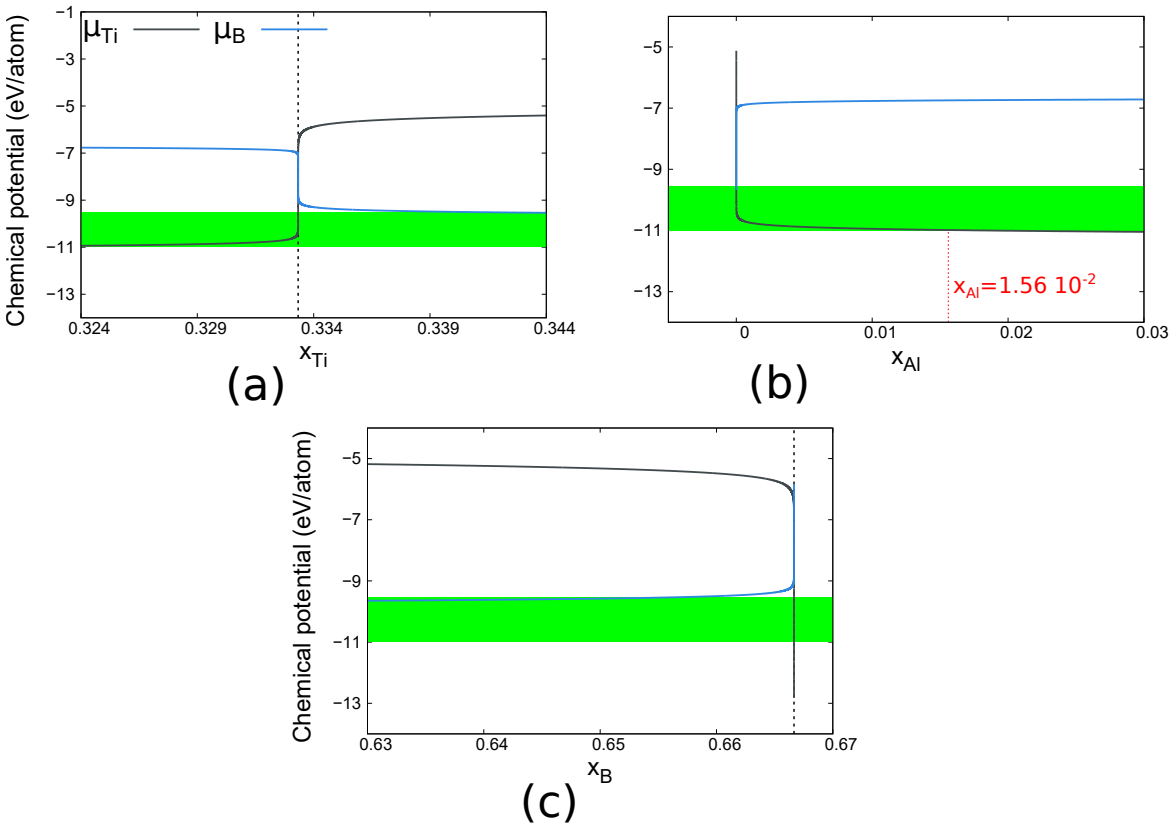

Fig. 8: IPDA-predicted Ti and B chemical potentials in TiB_2(Al) at 1000 K along the $\mu_{Al} = E_0$(Al) path, plotted as functions of the atomic fraction of each element in the compound. The green area has the same meaning as on Fig. 5.

yields detailed information on the phase compositions in the useful Al+TiB_2 domain, namely (see below) the so-called tie-line structure on a phase diagram. The required chemical potentials are displayed in Supplemental Material, in full 3D profiles and along the μ_{Al} = E_0(Al) path, which confirms our previous conclusions (0 K analysis, Fig. 6) that Al+TiB_2 equilibrium implies μ_{Ti} and μ_B lying in a sharp, thus high-sensitivity, zone. For further analysis, Fig. 8 displays μ_{Ti} and μ_B in a more convenient form, together with the stability domain introduced previously for the two-phase Al+TiB_2 system and expressed in terms of μ_{Ti} (green area), refining our previous picture of TiB_2 as stoichiometric compound when equilibrium with the fcc Al(B,Ti) solid solution is involved: (i) the B amount in TiB_2(Al) is fixed to 2/3 (Fig. 8(c)), and thus the Ti amount cannot exceed 1/3 (Fig. 8(a)); (ii) the Al solubility in TiB_2 should remain small (less than 2 %) (Fig. 8(b)). As demonstrated below, collecting these features will be useful to draw a fully atomic-scale-predicted Al-B-Ti phase diagram, and infer practical consequences on phase stability in Al-based MMCs.

3.3. IPDA to resolve controversies on AlB_2(Ti)

Owing to its utmost importance in Al alloys, the primary focus in our investigations is obviously on TiB_2, and indeed the analysis reported hitherto is sufficient to yield the thermodynamic properties in the two-phase Al+TiB_2 domain typical of such alloys, as will be shown in the next section. It is however of interest to include the AlB_2 compound in the current IPDA investigations of Al-B-Ti, at least for several reasons. Firstly, while AlB_2 should be avoided in TiB_2-strengthened Al alloys, it may nevertheless be observed in specific elaboration conditions, but currently available phase diagrams derived from phenomenological thermodynamics [22] are insufficient to predict reliably its behaviour in thermodynamically equilibrated real alloys. Secondly, the picture of AlB_2 as a nearly-stoichiometric compound suggested by these phenomenological phase diagrams seems to disagree with recent atomic-scale explorations [13, 14].

Despite the different electronic properties of aluminium and titanium, AlB_2 is almost completely isostructural to TiB_2, apart from slightly changed lattice parameters. This structural similarity of both metallic borides is a remarkable feature, and IPDA offers an easy way to check whether this may translate into similar PD and thermodynamic properties. It should be noted first that AlB_2 is very much less stable than TiB_2, its formation energy being -0.129 eV/formula unit compared to -3.174 eV/fu for TiB_2 (from the energies in Section 2.1), which is striking by itself and may be a part of the explanation to the very different defect chemical behaviours of these two compounds, as

emphasized below. To investigate this in more detail, the total and GC energies pertaining to PDs were calculated (see Supplemental Material) for AlB_2(Ti) with Ti additions, including the possibility of interstitials on (1b;2c;3f;3g) sublattices for all species, while in analogy with the aforementioned trends for Al in TiB_2, this possibility was neglected for Ti in AlB_2.

3.3.1. AlB_2 with Ti additions: 0 K analysis

For reasons that will become obvious below when inspecting non-zero temperatures, it is instructive to proceed for AlB_2 slightly differently from TiB_2, and consider first the PD properties of AlB_2 at T = 0 K. Besides, although less important than Al in TiB_2, Ti additions in AlB_2 will be included in the analysis, for the sake of completeness in the context of ternary Al-B-Ti, and also because the approach may be relevant for other additions (Cu, Mg,...) present in practical Al-based alloys. Fig. 9 shows that the PD properties of AlB_2(Ti), in the low-T range (T = 0 K limit), are significantly different from those obtained for TiB_2(Al). As an important qualitative discrepancy, only the x_B = 2/3 threshold is predicted in the (x_B;x_{Ti}) composition plane, the x_{Al} = 1/3 line corresponding then to no noticeable changes in the compound PD properties. Furthermore, Ti additions in AlB_2 should have a simpler behaviour than Al in TiB_2, as Ti is found to substitute on Al sites whatever the composition. This clearly illustrates the strongly different behaviours of both borides with respect to addition elements. Moreover, as concerns intrinsic PDs (x_{Ti}=0 baseline of Fig. 9), the T = 0 K analysis suggests that AlB_2 is quite distinct from TiB_2 clearly identified as a vacancy-type compound above: whereas Al depletion requires Al vacancies, Al excess is accommodated by Al antisites rather than B vacancies, suggesting that AlB_2 should belong to the class of triple-defect compounds, which near stoichiometry accommodate temperature increases by simultaneous formation of one antisite and two vacancies, hence a net PD formation which for AlB_2 can be written as [Al_B+2V_{Al}]. Finally, comparing the constant thresholds of chemical potentials predicted for AlB_2 in the 0 K limit (Fig. 9) to the μ_{Al} = E_0(Al) = -3.748 eV/atom value taken throughout as a reference characterizing the surrounding Al-based solid solution, clearly suggests that any Al+AlB_2 equilibrium should involve significant Al depletion in the compound. This issue will be considered further below including temperature effects.

3.3.2. Binary AlB_2: effect of temperature and phase equilibria

In principle, similarly to TiB_2(Al), the knowledge of the properties of AlB_2(Ti) was required for our general purpose of multiphase equilibria in Al-B-Ti. However, the finite-temperature analysis of

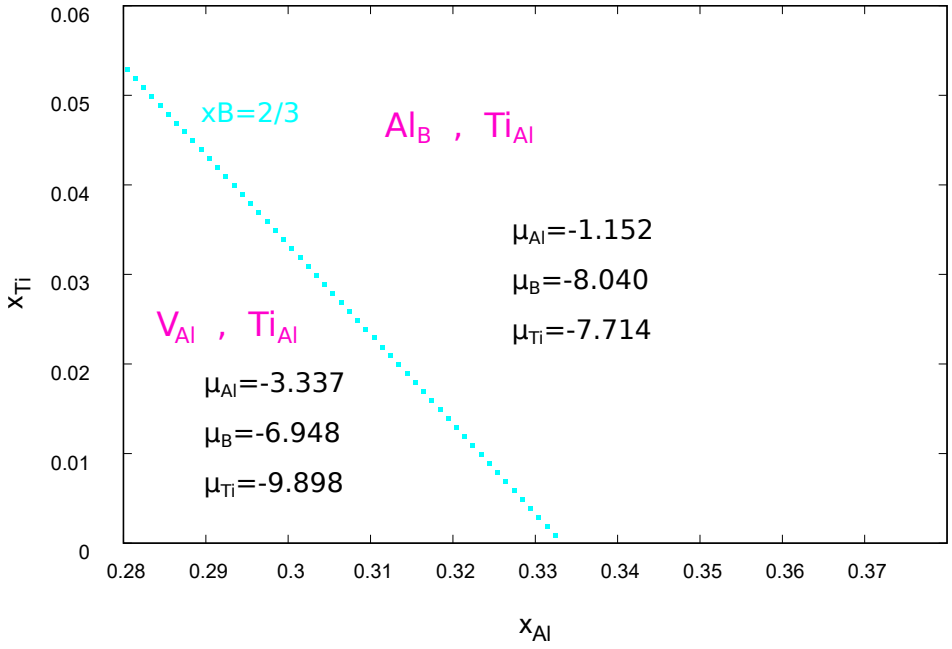

Fig. 9: PD properties of AlB_2(Ti) with Ti additions in the T = 0 K limit, from ab initio calculations and IPDA thermodynamics. The structural PDs and elemental chemical potentials (eV) are indicated in each composition domain.

AlB_2 was eventually not carried out in presence of Ti, as justified by the findings reported now. The IPDA analysis of Ti-free AlB_2 at 1000 K (Fig. 10) reveals that the behaviour of PDs in AlB_2 should be much more complex than previously predicted in the T = 0 K limit, thus more intricate than in TiB_2. On the whole, whereas in the Al-depleted domain the PD structure is rather simple - Al vacancies being strongly dominant at working temperatures - the intricacy is higher for Al excess, a competition occurring between Al antisites and B vacancies in this composition range. This feature strongly questions the belonging of AlB_2 to the aforementioned class usually referred to as triple-defect compounds: Fig. 10(c) shows that the usual triple defect [Al_B+2V_{Al}], expected from the 0 K analysis, loses its relevance as the temperature increases, AlB_2 becoming a vacancy-type compound with [V_B+V_{Al}] as characteristic combination of defects at stoichiometry. The IPDA analysis thus depicts AlB_2 as a compound with "hybrid" behaviour between the vacancy and triple-defect common classes, due to a strongly temperature-dependent PD structure. In addition, the intricacy of this structure is also enhanced by the simultaneous presence of Al_B and V_B as dominant defects in B-depleted compounds.

As a consequence, the additional presence of B vacancies, as non-structural but thermally prevalent PDs, may lower the validity of simplified pictures used previously [32] to yield analytic approximate expressions for PD formation energies in ordered compounds, and shown above to work reasonably well for TiB_2 (the analytic-IPDA approximations indicated on Fig. 3). In particular, the common result of equal formation energies for both kinds of structural defects at stoichiometry may no longer be valid for AlB_2. It should also be noted that this simultaneous presence of two major defects, namely Al_B and V_B, in Al-rich AlB_2 may increase the intricacy of the possible interactions between them, giving rise to a wider panel of possible complex PDs involving antisites and/or vacancies. Exploring the role of complex PDs is however a significant task in itself [33, 34], and is thus left for future works, when necessary, for some Al-B-Ti phases probably including AlB_2. As regards self-interstitials in AlB_2, Fig. 10 indicates they are minor PDs, occurring in negligible amounts with the same order of magnitude as B antisites. On the whole, provided complex PDs can be overlooked, these results suggest that TiB_2 and AlB_2 thus behave quite similarly for interstitial defects, involving either B or the metallic element constitutive of the compound, namely that these defects should be negligible in both borides. Such a conclusion is somewhat unexpected, and can obvioulsy not be generalized to other compounds with complex crystal structures involving both metallic and non-metallic elements (see e.g. an earlier work [11] on chromium carbides).

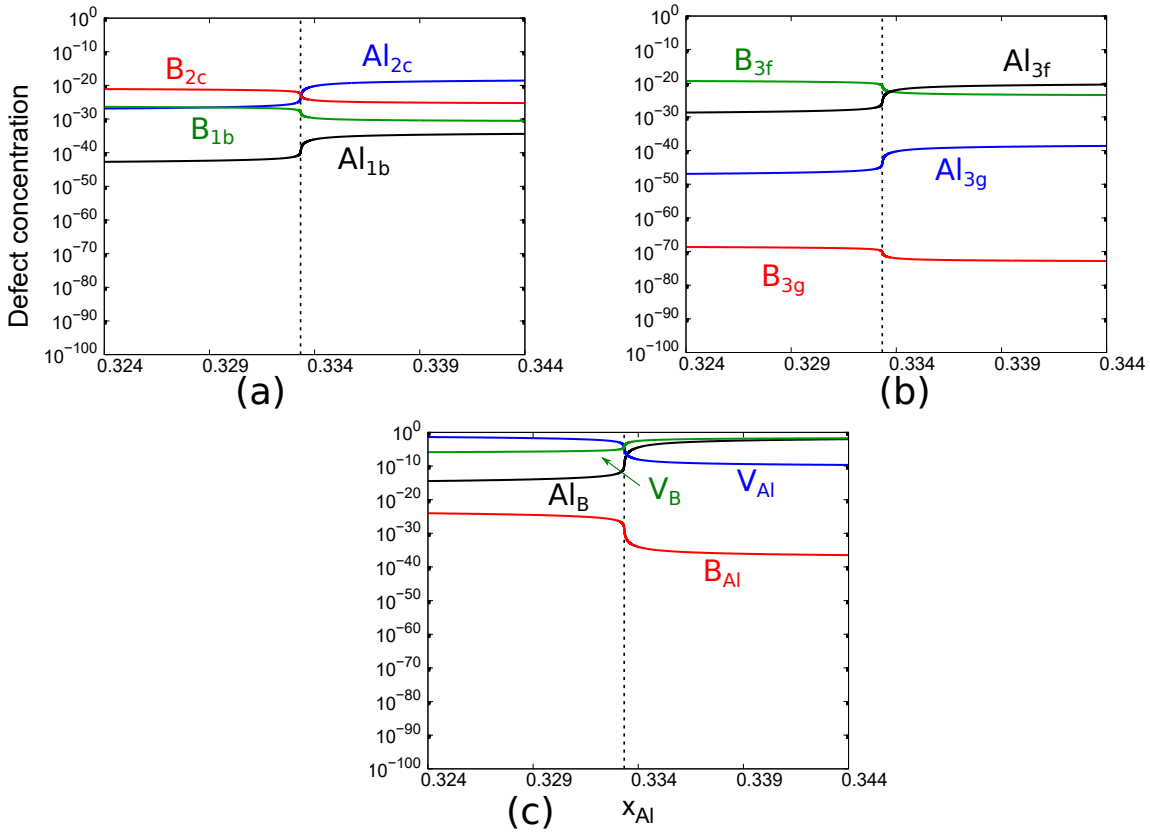

Fig. 10: Concentrations of PDs in AlB_2 from IPDA thermodynamics at 1000 K, including vacancies, antisites and interstitial defects.

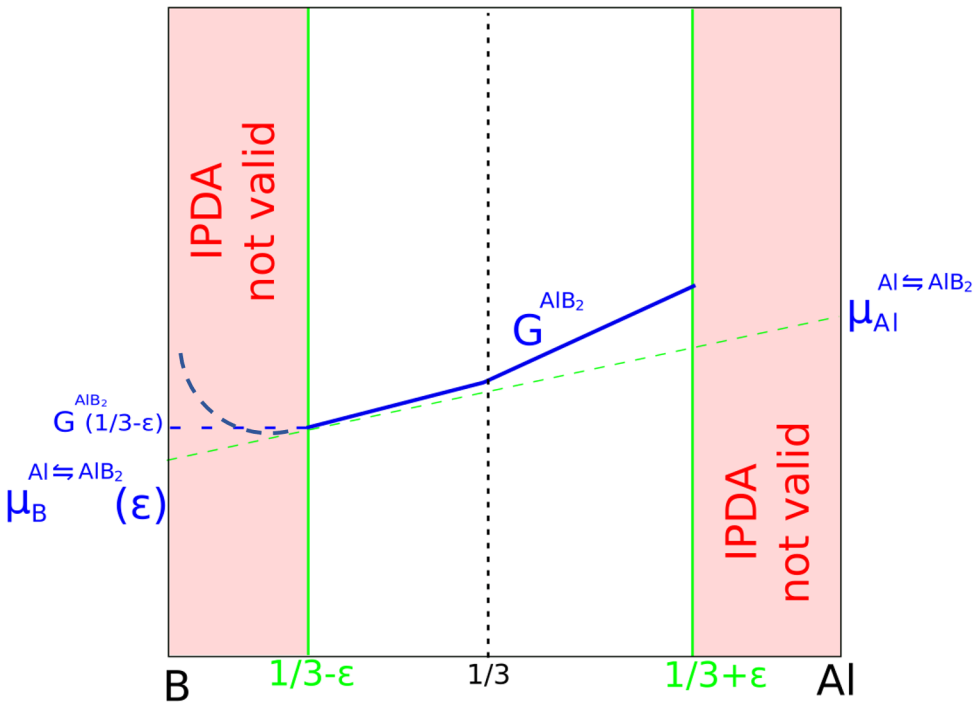

Fig. 11: Schematic Al-B free energy diagram, illustrating the significant Al-poor off-stoichiometry (with magnitude ε) of AlB_2 in equilibrium with fcc Al, thus located beyond the limits of IPDA validity (red areas). The dashed green line sketches equilibrium with the fcc Al solid solution. The two-phase Al equilibrium chemical potential $\mu_{Al}^{Al \leftrightharpoons AlB_2}$ is assumed to be equal to E_0(fcc-Al) specified in the methodology section.

The free energy of AlB_2 derived from these IPDA results is depicted on Fig. 4(b), indicating a monotonically decreasing profile, i.e. a behaviour strongly different, on the B excess side of stoichiometry, from that previously obtained for TiB_2. While the validity of this prediction can hardly be assessed in itself, a much broader insight is gained when replacing this free energy profile within a larger scope of Al+AlB_2 equilibrium, namely by confronting it with the energy level of fcc Al. Confirming our previous remark drawn from Fig. 9, this situation is sketched on Fig. 11, which suggests that, contrary to earlier calculations [22], no equilibrium can be found, within the present IPDA scheme, between nearly stoichiometric AlB_2 and Al at working temperatures. Nevertheless, the validity of IPDA being usually restricted to moderate (a few atomic %) departures from stoichiometry, beyond which interactions between PDs should begin to be unavoidable, it may be expected that this Al-depleted off-stoichiometry threshold (noted ε on Fig. 11) should correspond to an increase - not captured by IPDA - of the AlB_2 free energy profile, thus allowing to recover a common tangent required for equilibrium with Al to settle. As a consequence, phase equilibria in TiB_2-reinforced Al alloys should involve Al-depleted off-stoichiometric AlB_2 with strong amounts of structural Al vacancies, at odds with the predictions drawn from current phenomenological models [22, 13, 14] viewing both AlB_2 and TiB_2 as purely antisite compounds. Furthermore, this strong tendency to Al depletion in AlB_2 questions the validity of the B chemical potential range (eq. 15, section 2), as deduced previously from the simplifying assumption of stoichiometric defect-free phases. Our results indicate that this assumption probably fails for AlB_2. Most critically, in view of the aforementioned issues on the reliability of predicted phase diagrams (e.g. for Al-B-Ti) involving complex phases, the present study of AlB_2 clearly demonstrates the role of IPDA as an efficient tool to identify possible deficiencies and suggest improvements when designing phenomenological models for the thermodynamic properties of ordered compounds. To conclude this section, it must be pointed out that, owing to the previous restrictions on this compound, the 3D free energy of AlB_2(Ti) is displayed for completeness on Fig. 2 (green color), but will not be used in the subsequent analysis of phase equilibria.

3.4. IPDA and multiphase equilibria in Al-B-Ti: comparison with experiments

The previous IPDA-based thermodynamics of the Al(B,Ti) solid solution and both metallic borides allows, through a proper upscaling from the atomic level, to investigate macroscopic current open issues on multiphase stability in Al-based MMCs. Owing to the aforementioned restrictions for AlB_2,

and while the IPDA modelling revealed no failure in itself, a broader picture encompassing phase equilibria was found to lead to exceedingly large Al depletion in AlB_2, suggesting that the IPDA model for this compound should deserve further refinements (see below in Discussion). Therefore, our investigations are focused on the two-phase equilibrium between Al(B,Ti) and TiB_2(Al). AlB_2 is thus treated on an equal footing with Al_3Ti, namely as two perfectly ordered compounds, the role of which is merely to delimit the TiB_2(Al)+Al(B,Ti) two-phase domain. In this context, the relevant part of the Al-B-Ti phase diagram (isothermal section at 1000 K), as derived from the IPDA modelling of Al(B,Ti) and TiB_2(Al), is displayed on Fig. 12, and provides a convenient tool for our further investigations of Al-based MMCs. Due to the low solubilities of addition elements in both phases, the scale on this figure was not respected for clarity, the actual equilibrium compositions being given in Table 1. On the whole, using the methodology described in section 2, the IPDA-predicted Al+TiB_2 two-phase domain, delimited by the bold green tie-lines associated with occurrence of either AlB_2 or Al_3Ti (respectively $\Delta\mu_{Ti}$=-3.043 eV or -1.594 eV on figure 12, see eq. 14), is found to show a characteristic structure made of a pair of "head-to-tail fans" of intermediate tie-lines, located on each side of the $x_B=2x_{Ti}$ isopleth (red dashed line). While such overall features, conveniently derived from the IPDA atomic-scale analysis, can be fruitfully employed to improve phase diagrams built from more phenomenological approaches, useful quantitative trends of Al(B,Ti)+TiB_2(Al) equilibrium (Table 1) are also worth mentioning, which can be related to the properties of two-phase Al-based alloys containing TiB_2 particles. Considering first the Al(B,Ti) solid solution, the solubility of B in this phase across the two-phase domain remains negligible, typically below one ppm, at working temperatures. This however does not preclude a noticeable influence of B, since this element is known to strongly segregate at interfaces such as grain boundaries. As regards Ti solubility, it is found to increase drastically, from negligible values to roughly 1 at. %, when going from the AlB_2 limiting line to the Al_3Ti one, a property thus strongly depending on the overall composition of the - supposedly two-phase - alloy (see next paragraph for further remarks on this topic). Turning then to TiB_2, the solubility of Al in this phase shows large variations across the two-phase domain, from negligible to much more significant values (1.5 at. %). The consequences of these features on the practical properties of Al-based MMCs may be rather subtle, including changes of the TiB_2 particles themselves, e.g. via the Al-dependence of the elastic field associated to the (semi-)coherent interfaces beteen both phases. It is noteworthy that the previous theoretical analyses of Al|TiB_2 interfaces [15, 16], assimilating TiB_2 to a perfect (i.e. defect-free

and Al-free) compound, have totally overlooked these aspects. Moreover, since Al solubility in TiB_2 was previously found to occur mainly by Al substitution on Ti sites, its variation induces noticeable changes (up to 1.5 at. % off-stoichiometry) in the Ti content of the compound, with negligible influence on the B content which remains close to 2/3 throughout the two-phase domain.

Tab. 1: From ab initio IPDA thermodynamics, compositions (1000 K) of the TiB_2(Al) compound and Al(B,Ti) solid solution, for both limiting cases of three-phase equilibria corresponding to the formation of a third neighbour phase, either Al_3Ti or AlB_2, as specified in the first row of the Table. The chemical potentials (eV) are also recalled for both three-phase systems.

	Al_3Ti formed		AlB_2 formed	
T=1000 K	Al(B,Ti)	TiB_2(Al)	Al(B,Ti)	TiB_2(Al)
μ_{Al}	-3.748		-3.748	
μ_{Ti}	-9.540		-10.989	
μ_B	-7.470		-6.744	
x_{Al}	99.6 %	0.8×10^{-9}	$\approx$ 100 %	1.5 %
x_{Ti}	0.4 %	$\approx 1/3$	0.2×10^{-9}	31.7 %
x_B	0.5×10^{-10}	$\approx 2/3$	0.2×10^{-6}	$\approx 2/3$

Going one step beyond these IPDA-predicted intrinsic features of Al-B-Ti phase diagrams, the present study also yields farther-reaching practical comparisons with Al-based MMCs reinforced by TiB_2 particles, e.g. those alloys designed from 7075Al series. The improved mechanical properties of these MMCs are ordinarily attributed to TiB_2 particles, which are supposed to entail a beneficial grain refinement, and are introduced into an initial Al liquid bath at some level of a complex multi-step elaboration sequence. As often in elaboration processes, the design of these alloys involves ill-controlled and ill-understood transient formations or disappearances of phases, which suggests interesting attempts of interpretation using the present IPDA work. To be more specific, the required addition of TiB_2 into the MMC is frequently carried out by means of a "master-alloy" or "grain refiner", the most frequent of which is the ternary alloy Al-5Ti-1B (in wt.%, i.e. 2.8 and 2.5 at.% of Ti and B respectively). Among the ongoing debates about grain refinement and related mechanisms, mostly intriguing is the controversial status of the Al_3Ti intermetallic compound limiting the Al+TiB_2 two-phase domain (Fig. 12), during elaboration as well as in final MMCs. While it has even

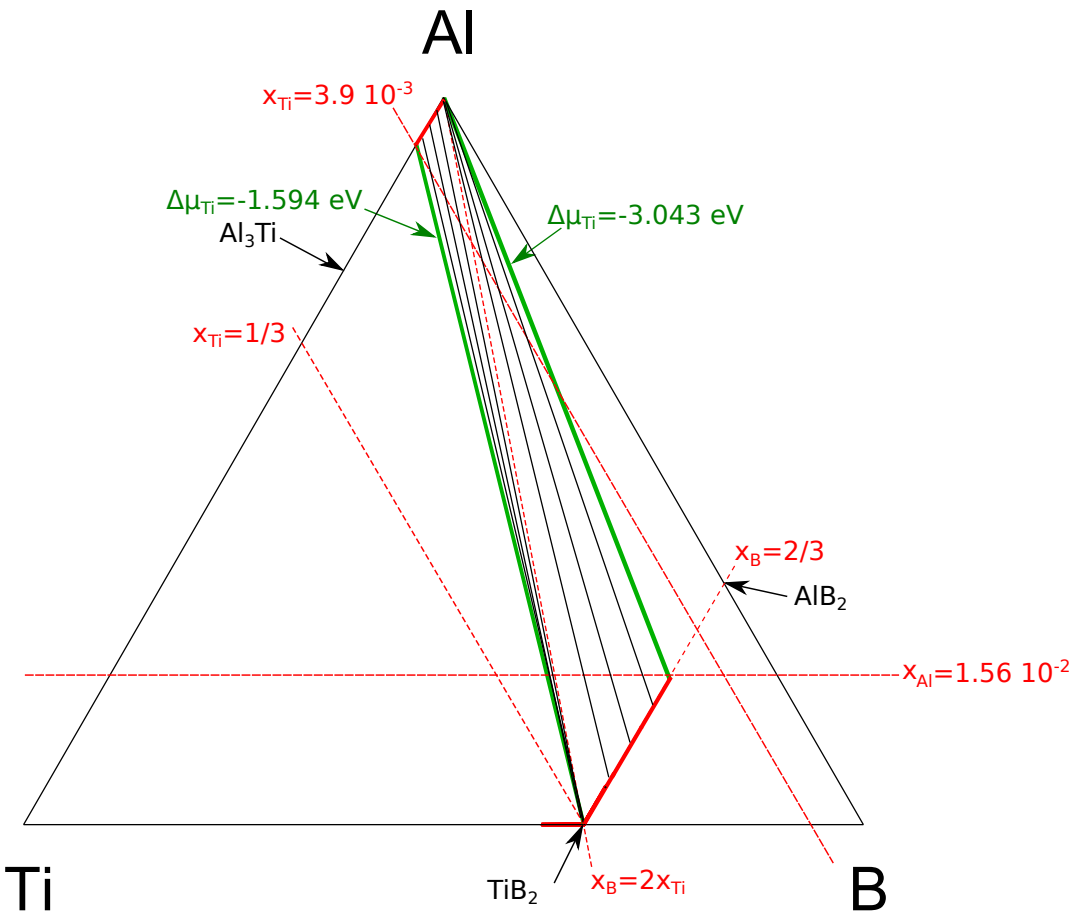

Fig. 12: Schematics of the calculated (ab initio-based IPDA thermodynamics) isothermal section (1000 K) of the Al-B-Ti phase diagram (scale not respected), showing the whole Al+TiB_2 two-phase domain.

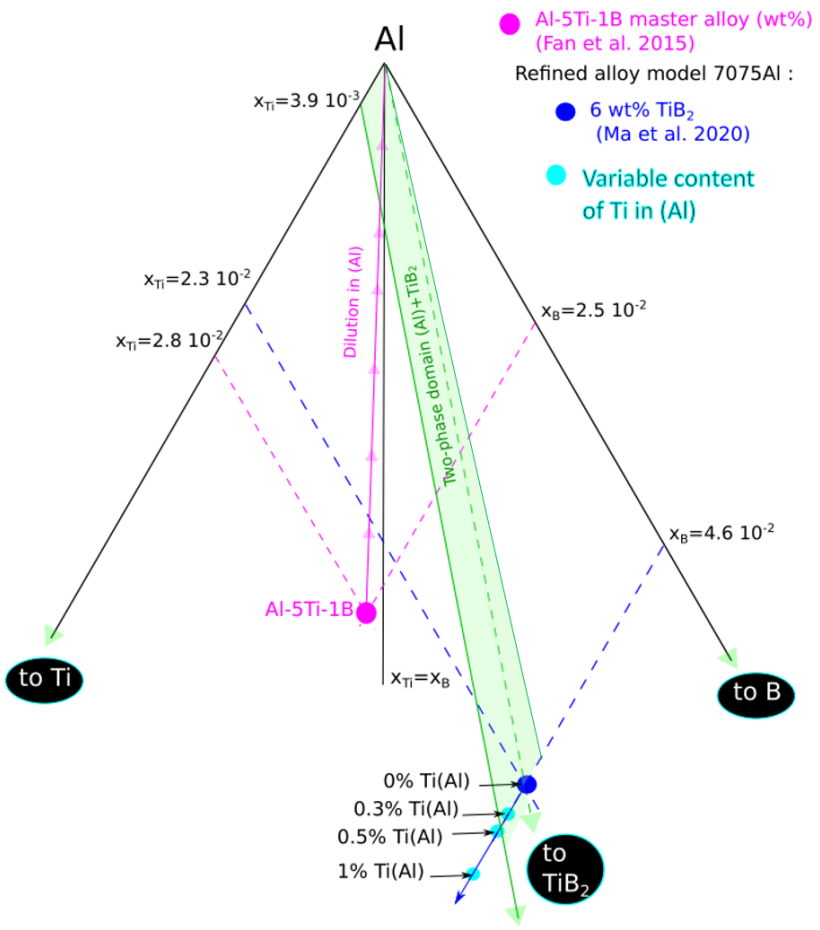

Fig. 13: True-scale representation of the Al corner of the same phase diagram, including (i) the frequently employed [35] Al-5Ti-1B master alloy (purple dot), and (ii) a grain-refined 7075Al alloy containing 6 wt. % TiB_2 [17] (blue dot); in the latter case, (iii) the effect of additional Ti in solution in the Al matrix is also displayed (light blue dots).

been suggested - a striking assumption - that grain refinement could be due to Al_3Ti rather than to TiB_2, the structure and stability of Al_3Ti in themselves raise valuable questions. Noticeably, it is not clear whether this compound appears in bulk form, or as a two-dimensional layer at the $Al|TiB_2$ interfaces. Moreover, whereas Al_3Ti can be detected in the ternary precursor Al-5Ti-1B [35], this compound is seemingly absent from the final strengthened grain-refined alloys, where only a Laves phase $Mg(Cu,Zn)_2$ is observed at $Al|TiB_2$ interfaces [18]. On the whole, the factors, either thermodynamic or kinetic, controlling this (dis)appearance of Al_3Ti during the elaboration process are still to be elucidated. In this context, in order to bring reliable thermodynamic arguments for interpretation, it is instructive to focus on the Al corner of the Al-B-Ti phase diagram, derived from the present atomic-scale investigations, which for quantitative analysis is displayed at true composition scale on Fig. 13. As a first interesting trend, stemming from the low solubilities and limited size of the $Al+TiB_2$ two-phase domain, the representative point (purple dot) of Al-5Ti-1B on this diagram is found to lie within the $Al+Al_3Ti+TiB_2$ three-phase domain, in good agreement with the previously mentioned experimental presence of Al_3Ti in this master alloy. Secondly, Fig. 13 also shows (purple arrows) that the moderate "distance" in composition space, separating Al-5Ti-1B from the $Al+TiB_2$ two-phase domain, can be covered easily if Al-5Ti-1B is diluted into a larger Al-based alloy candidate to grain refinement. Here again, the trend predicted from our atomic-scale study agrees well with the experimental absence of Al_3Ti in final grain-refined alloys. Remarkably, this dilution-induced shift into the two-phase domain directly results from the non-negligible amounts of Ti accepted by the (Al) solid solution, a feature predicted by IPDA modelling and overlooked if stoichiometric phases were assumed. This agreement between atomic-scale thermodynamics and experiments can even be illustrated further on a grain-refined 7075Al alloy elaborated for experimental studies [17]. In this case, the inoculation process did not pass through the Al-5Ti-1B master alloy but proceeded by directly adding B- and Ti-containing salts, thus forming directly TiB_2, the weight fraction of which (6 wt.%) is indicated in Ref. [17]. Whereas this alloy was thoroughly investigated [18], this did not reveal any presence of Al_3Ti. Noticeably, the absence of Al_3Ti in this grain-refined Al-based MMC is roughly confirmed by our calculations, since the point corresponding to this alloy (deep blue dot on Fig. 13) falls within the $Al+TiB_2$ two-phase domain, a consequence from the IPDA-predicted significant solubilities of Ti in (Al) and Al in TiB_2. Fig. 13 (light blue dots) indicates that up to 0.3 at. % Ti in (Al) is an acceptable amount if Al_3Ti formation is to be avoided. Moreover, while the respective proportions of the various salts in this process should in general

imply some excess of Al_3Ti or AlB_2, the Al+TiB_2 two-phase domain present on either side of the Al-TiB_2 line on Fig. 13 allows (to a certain extent) to avoid the presence of these compounds in the final alloy. To conclude this section devoted to comparison with practical alloys, the present work on Al-B-Ti demonstrates that atomic-scale IPDA-based thermodynamics offers a convenient tool to help elucidating experimental issues, such as the controversial behaviour of the Al_3Ti compound in Al-based alloys refined by TiB_2.

4. Discussion

As demonstrated above from its application to aluminium alloys, the proposed IPDA approach for atomic-scale thermodynamics provides an efficient tool to explore alloy stability in multiphase environments, especially when complex crystal structures are at stake. It allows building accurate phase diagrams including a deep level of details (tie-lines...), which constitutes a practical strength to carry out various comparisons with other, more phenomenological (e.g. Calphad-type), predictions from computational thermodynamics. While the (apparent) deficiency of IPDA application to AlB_2 suggests that a more sophisticated atomic-scale thermodynamic modelling might be required specifically for this compound, this does however not question the relevance of the overall approach to investigate multiphase alloy equilibria. In particular, a recent work [13], using cluster expansions and Monte-Carlo simulations, was devoted to an atomic-scale study of $Ti_{1-x}Al_xB_2$, leading to predict phase-separation trends between both borides. In spite of its wide scope, this study was carried out under the assumption that transitions between borides occur exclusively via Ti vs Al substitutions on the metallic sublattice, thus considering B atoms as "spectators", a hypothesis chosen to enhance the tractability of cluster expansion thermodynamics, much more cumbersome than IPDA. Likewise, it is worth mentioning another recent study [14], devoted to atomic-scale investigations of metal-deficient $Al_{1-\delta}B_2$, and suggesting that, due to an intricate behaviour of Al vacancies, this compound should display a narrow composition range of stability and some significant (2 at.%) Al-depleted off-stoichiometry, in agreement with our previous remarks on the possible limitations of IPDA for AlB_2 (see Fig. 11). As for ref. [13], the conclusions of this earlier work [14] on AlB_2 were drawn within the hypothesis of "spectator" B atoms. In this respect, our IPDA study of Al-B-Ti is complementary to each of these previous investigations on metallic borides, since it properly includes all kinds of point defects and departures from stoichiometry, and allows for an easier capture of subtle effects due to addition elements in borides (e.g. Ti in AlB_2). In particular, in the Ti-B

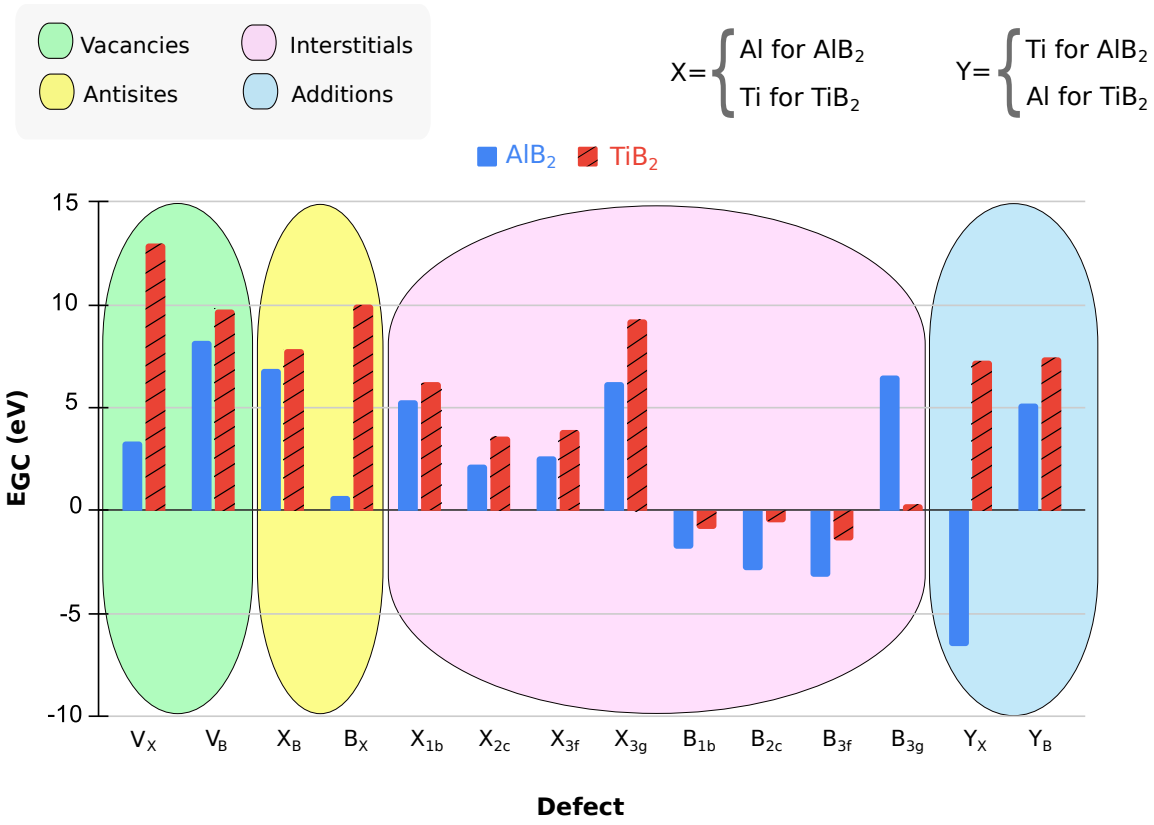

Fig. 14: Comparison of GC energies of intrinsic and addition PDs in TiB_2(Al) and AlB_2(Ti), from ab initio calculations.

system, this approach predicts that TiB_2 is a vacancy compound, which is at odds with its Calphad description adopted so far [20, 21]. Our work then suggests to revisit the models adopted for the diborides in this type of approach and to assess the impact of such modifications on the obtained phase diagram. Finally, it is worth noting that the calculated phase and defect energies could be expressed as Calphad models using the compound energy formalism (CEF). Standard Calphad software could then be used to easily generate the phase diagrams (and compare to Figs. 12 and 13), a probably fruitful task left for future works.

There is a long-standing controversy [36] concerning TiB_2 and AlB_2 since they have the same

structure: do TiB_2 or AlB_2 exist as two separate phases or as a continuous series of solid solutions, $(Al_xTi_{1-x})B_2$? Our study on TiB_2 clearly shows that its Al solubility limit is quite limited and not higher than approximately 1.5 at %. Beyond this value, there is formation of AlB_2 (cf. Table 1, eqs. (13)-(16) and related comments at end of section 2 and beginning of section 3.4). This result is in accordance with previous experimental and numerical works [36, 13], in which a low solubility of Al in TiB_2 and Ti in AlB_2 was evidenced, a continuous compound (Al,Ti)B_2 being then not stable. A measured value of x = 0.01 was reported [36] which is slightly lower than the solubility limit calculated in this work (x = 0.045) but of the same order of magnitude. Considering the underlying assumptions, the agreement is satisfactory, which shows that the IPDA grasps the main thermodynamic features of the Al-B-Ti system.

The current IPDA study of metallic borides has revealed strongly different point-defect-related behaviours between AlB_2 and TiB_2, in particular the fact that the IPDA free energy for AlB_2 allows no equilibrium with the Al solid solution, whereas IPDA modelling of TiB_2 is straightforward. Elements to understand these discrepancies are provided by comparing the GC energies of all intrinsic PDs in both borides. To this purpose, comparing the full overviews of GC energies is mandatory, since GC energies of PDs taken separately are meaningless quantities. From Fig. 14, it appears that the main discrepancy comes from PDs, vacancies and B antisites, on the respective metallic sublattices. These PDs, responsible for Al or Ti depletion, are much less energetic (with respect to other kinds of PDs) in AlB_2, hence the enhanced stability of AlB_2 (with respect to TiB_2) for metal-depleted off-stoichiometry ($x_{Al}<1/3$), a trend in good agreement with previous conclusions [14]. Another non-negligible discrepancy between the PD structures of TiB_2 and AlB_2 can be noted for B_{3g} interstitials, much less favourable in AlB_2. However, due to the minor character of self-interstitials in both borides, this difference is not relevant to interpret the free energy profiles, and a similar remark holds for B_X antisites (X = metallic element). In order to get a deeper insight into the intricate behaviour of AlB_2, it is thus legitimate to focus on the effect of aluminium vacancies V_{Al}. Fig. 4(b) shows (mixed blue lines) that increasing the GC energy of this peculiar PD may indeed be sufficient for equilibrium between fcc Al and nearly stoichiometric AlB_2 to be recovered. The required rise of vacancy GC energy (roughly 1 eV) may be easily attainable if refinements were included in IPDA, in particular those due to PD phonons, as demonstrated by the significant phonon-induced increases of vacancy GC energies previously obtained in the case of nickel aluminides [37] (see below for additional remarks on PD phonons). However, since phonon contributions with unknown magnitudes

are expected for various types of PDs, more reliable conclusions on the relevance of IPDA to capture equilibria involving AlB_2 would require full account of these additional contributions, which is left for future work.

In this context, it is highly relevant to further discuss two main factors that have been neglected in the above IPDA study of AlB_2, namely (i) point defect phonons, and (ii) complex point defects, both being likely to modify the PD and related thermodynamic properties of this boride. As regards issue (i), atomic-scale investigations of PD phonons in ordered compounds still remain critically scarce in general [38, 39, 37, 40]. While phonons in metallic borides are largely unexplored hitherto, a significant influence should be expected, in analogy with hydrogen-induced phonon effects widely recognized in hydrides [40], since boron is a light element. At this stage, earlier works on $NiAl_3$ and Ni_2Al_3 nickel aluminides [38, 37] have already allowed to delineate general trends, valid at least in these intermetallic compounds, of phonon GC free energies F_{GC}^{ph} as function of the various kinds of intrinsic PDs, namely F_{GC}^{ph}(interstitials) $< F_{GC}^{ph}$(antisites) (≈ 0) $< F_{GC}^{ph}$(vacancies). The high discrepancies predicted then among PDs of different kinds, reaching ≈ 1 eV at 1000 K, strongly point out a prominent influence of phonons on the PD structures and derived phase equilibria. While these conclusions rather pertain to Ni-based alloys, similar analyses would be useful for compounds, such as metallic borides, involved in other kinds of widely used alloys, e.g. Al-based ones. More generally, since current computational facilities make it easy to include phonon contributions in atomic-scale thermodynamics, such a task would be particularly valuable for the numerous compounds, poorly explored up to now, involving metals and non-metallic elements (borides, nitrides...). As regards (ii) complex PDs, this issue would also deserve further attention in metallic borides, especially owing to the possible formation of boron-vacancy complexes, the latter being well-known to exist e.g. in B-doped iron aluminides FeAl(B) [33]. More recently, the role of complex PDs was thoroughly explored in oxygen-doped titanium aluminide TiAl(O) [34]. However, the thermodynamic consequences, for multiphase stability, of complex PDs involving boron or oxygen were investigated in none of these two studies.

Due to the utmost practical interest of equilibria between fcc-based aluminium matrices and TiB_2 strengthening particles in the context of Al-based MMCs, the present work mainly illustrates the exploration of a selected part of the Al-B-Ti phase diagram around the Al+TiB_2 domain. However, the proposed ab initio IPDA-based approach for atomic-scale thermodynamics easily lends itself to much wider explorations. For Al-B-Ti, in addition to AlB_2 already discussed, this mainly

concerns the zone along the Al-Ti axis, and several Al-Ti ordered phases could be included fruitfully, to provide an exhaustive phase diagram. Among these phases, Al_3Ti is probably the most relevant one, due to its proximity with fcc-based Al solid solutions in composition space. While Al-Ti ordered compounds have already formed the subject of numerous atomic-scale investigations [34], a single work was devoted to Al_3Ti [41], with focus on point defect properties, but this earlier work could not be taken into account in the present investigations of Al-B-Ti, since (i) its conclusions were derived from a questionable picture of the compound, one Al sublattice being overlooked without justification, and (ii) the effect of boron additions was not explored. On the whole, wider applications of IPDA thermodynamics to B-doped Al-Ti ordered phases, allowing to fill the unexplored domain located around the Ti corner of the Al-B-Ti phase diagram (Fig. 12), should provide informative future works on Al-based alloys. Likewise, another noticeable strength of IPDA thermodynamics, allowing many future extensions, lies in its ability to explore the influences of the numerous addition elements involved in elaboration processes. For aluminium alloys, key issues are related to the trends of additions to incorporate the TiB_2 strenghtening particles, or other phases such as the $Mg(Zn,Cu)_2$ compound experimentally observed at $Al|TiB_2$ heterophase interfaces [18].

While designed primarily to explore bulk properties of multiphase alloys, IPDA thermodynamics may also efficiently help improving the description of microstructural elements in these complex systems, especially for grain boundaries and heterophase interfaces. As demonstrated by the wealthy literature devoted to atomic-scale studies of interfaces, the bridge here must be settled on the elemental chemical potentials, key quantities which are usually difficult to obtain and easily derived in the IPDA framework. As well known from the Gibbs phase rule, if the number of elements exceeds the number of phases, which is by far the most current case in practice, the chemical potentials in multiphase multi-element alloys at equilibrium generally depend on the overall composition. This issue drastically enhances the intricacy when studying interfaces, mostly because excess energies of interfaces, parameters controlling interface stability, cannot be regarded as intrinsic features. Conversely, equal numbers of elements and phases correspond to a remarkably favourable situation for atomic-scale studies of interfaces, due to the absence of dependence upon overall composition. In this situation, the chemical potentials can straightforwardly be derived from the bulk free energies of the phases, the derivation being made simpler by the assumption, conveniently overcome by IPDA, that both phases can be considered as perfect, i.e. by neglecting

all point defects and off-stoichiometries. As a consequence, due to practical constraints in simulations (periodic boundary conditions) atomic-scale studies of interfaces are usually carried out only between two phases, unambiguous interface energies can be reached only for binary alloys, namely for model systems quite far from real alloys. These restrictions explain the low amount of works hitherto dedicated to interface studies in complex alloys, especially when compared to two-phase binary systems forming the topic of numerous investigations, e.g. for widely used Ni-Al and Al-Cu intermetallics [42, 43, 44, 45, 46] or metal-hydride systems [47, 48]. In more complex cases, exclusively two-phase ternary systems so far (to our knowledge), inspection of the literature [15, 16, 31] shows that the common way to partially circumvent the difficulty consists in performing interface studies in a less accurate parametric form, i.e. by keeping several chemical potentials (a single one in practice for two-phase ternary systems) as free parameters and confining them to a reasonable range, the bounds of this interval being chosen to ensure that no undesired or unobserved supplementary phases are stable. Specifically for Al-B-Ti, considering interfaces between Al and TiB_2, inspection of the two limiting three-phase equilibria Al+TiB_2+AlB_2 and Al+TiB_2+Al_3Ti allows to determine "operative" domains for the chemical potentials, namely domains consistent with the stability of two-phase Al+TiB_2 ternary alloys, the treatment being usually simplified by restricting to perfect defect-free phases, as pointed out above [16, 19]. In this context, the IPDA thermodynamics framework illustrated above allows significant improvements for atomic-scale studies of interfaces in complex alloys, since the knowledge of the overall alloy composition allows selecting the unique "operative" set of chemical potentials, from which interface energies can then be derived without ambiguity, whereas the parametric approach can be discarded.

Checking the predictions of IPDA thermodynamics from experiments is a hardly feasible task if one considers the "raw" outputs of IPDA, namely the point defect structures of the various present phases, because reaching information on these low-scale properties requires intricate spectroscopic methods (EXAFS, XANES,...), themselves submitted to heavy models for interpretations. Conversely, this is a much easier task to produce experimental samples of alloys with well-controlled panels of addition elements and submitted to well-controlled heat treatments of equilibration, thus well suited for comparisons with IPDA-predicted multiphase equilibria. Nevertheless, as shown by the frame diagram (Fig. 1), the approach described above does indeed make no reference to experimental data, as it entirely relies on an ab initio-based IPDA thermodynamics modelling of the various phases. The only experimental data are those added on Fig. 13 for discussion. Similarly,

no external thermodynamic database is required in principle: it may however be noted that this favourable theory-based-only context (needing no "external boost", experimental or phenomenological) is somewhat related to the fact that we were interested in the properties of condensed, solid phases for which DFT provides a priori reasonable results. It is actually a well-known fact that the DFT modelling of gas phases (noticeably O_2) is less accurate. In such cases, earlier literature shows it is common practice to correct the DFT free energies and chemical potentials in the gas phase using phenomenological databases. The above set of arguments demonstrates that ab initio-based IPDA thermodynamics offers a convenient route to connect atomic-scale properties and thermodynamics for multiphase multi-element alloys involving structurally complex, low-symmetry compounds.

As regards equilibria in multiphase alloys involving many complex compounds, two directions may be identified to extend the present approach (as shown by the couple of parallel downward arrows at second step of the flowchart displayed on Fig. 1): (i) for systems with moderate phase and chemical dimensionalities, as illustrated in the present work, the analysis may be achievable fully at the atomic scale (left arrow), while (ii) for systems of higher complexity, a more convenient route (right arrow) may be to use the IPDA framework to calculate robust phase/defect Gibbs energies, and then formulate this as Compound Energy Formalism (CEF) models and use the Calphad tools to calculate phase equilibria [49, 50]. Moreover, a wider use of ab initio-based IPDA could provide an incentive to create and expand databases (possibly in connection with already existing ones, e.g. [51]) reporting on atomic-scale predictions of point defect and derived thermodynamic properties near stoichiometry, covering a large panel of compounds with arbitrary low-symmetry crystal structures [52] and various addition elements, thus allowing a more reliable handling of these frequently poorly characterized compounds in larger-scale simulations including non-equilibrium phenomena [53]. Finally, as such databases of IPDA-predicted properties of compounds would inherently include detailed information on sharp defect-related changes of behaviour around stoichiometry, they may be well suited to refine predictive models of other properties (e.g. diffusion, melting [54]) for which experimental reliable inputs are extremely difficult to obtain.

5. Conclusion

The origin of this work lies in a recurrent observation, namely that interpreting and predicting phase formation and stability in multiphase multi-element alloys involving structurally complex

compounds still currently constitutes a difficult task. This deficiency, mostly obvious in recently discovered complex systems such as multi-principal-element or high-entropy alloys, is also highly noticeable in more usual classes of alloys, such as iron- or aluminium-based materials. Indeed, the various elaboration processes of alloys usually entail, either transiently or permanently, the presence of numerous complex phases, whereas, in spite of valuable computational tools such as Calphad approaches, our ability to understand and control their - often undesired - formation remains limited by the accuracy of the phenomenological thermodynamic databases required as input in these approaches. Most critically, it is often hazardous to undertake, for these complex time evolutions of phases in elaboration processes, any interpretations in terms of kinetic arguments, as long as the predicted equilibrium states of these alloys remain crippled with strong uncertainties. In order to help overcoming these issues, the core of this work was the proposal of a robust methodology for atomic-scale thermodynamics, relying on ab initio density-functional calculations and the independent-point-defect approximation (IPDA), allowing to explore equilibrium states of various alloys with multiphase and multi-element environments.

To illustrate the proposed approach, we considered the practically interesting case of Al-based metal-matrix composites (MMCs) strengthened by TiB_2 particles, well approximated by the Al-B-Ti ternary system. The founding layer of our approach consisted in thorough IPDA investigations of the relevant phases in these aluminium alloys. While our main focus was on TiB_2 including Al additions, the AlB_2 compound, observed but undesired in practice, was also investigated, showing that TiB_2 and AlB_2, though isostructural, are characterized by unexpectedly diverging behaviours. Including the Al-based solid solution typical of fcc matrices in real alloys, our approach gave further insight into multiphase equilibria, through the Al-B-Ti phase diagram around the Al+TiB_2 two-phase domain mostly interesting for Al-based MMCs. This allowed us to interpret currently debated experimental observations related to Al MMCs, which could not be explained by earlier phenomenological approaches. Noticeably, these conclusions were obtained thanks to the proposed methodology for atomic-scale thermodynamics, which is physically justified and does not rely on phenomenological assumptions. These are two major advantages since such assumptions may turn out to become critically inaccurate when the chemical and structural complexities of the phases rise too much. This methodology can easily be transferred to more complex multiphase systems, and easily lends itself to extensions towards higher-order mixtures by including various addition elements, such as (Cu, Mg, Zn...) typical of real Al alloys, and also widely present in other classes

of complex materials such as multi-principal-element alloys.

Acknowledgements

The authors thank the Centre de Ressources Informatiques (CRI) of the Université de Lille for computational facilities.

Data availability

Input data related to this work can be found in supplemental material.

Bibliography

[1] P. Y. Chew and A. Reinhardt. Phase diagrams — Why they matter and how to predict them. *J. Chem. Phys.*, (158):030902 (19), 2023.

[2] R. Besson. Understanding phase equilibria in high-entropy alloys: I. Chemical potentials in concentrated solid solutions – Atomic-scale investigation of AlCrFeMnMo. *J. Alloys Comp.*, (872):159745, 2021.

[3] D. Sobieraj, J.S. Wróbel, T. Rygier, K.J. Kurzydłowski, O. El Atwani, A. Devaraj, E. Martinez, and D. Nguyen-Manh. Chemical short-range order in derivative Cr–Ta–Ti–V–W high entropy alloys from the first-principles thermodynamic study. *Phys. Chem. Chem. Phys.*, (22):23929, 2020.

[4] L. Holliger, A. Legris, and R. Besson. Hexagonal-based ordered phases in H-Zr. *Phys. Rev. B*, (80):094111, 2009.

[5] R. Besson, A. Legris, D. Connétable, and P. Maugis. Atomic-scale study of low-temperature equilibria in iron-rich Al-C-Fe. *Phys. Rev. B*, (78):014204, 2008.

[6] R. Besson, J. Dequeker, L. Thuinet, and A. Legris. Ab initio thermodynamics of complex alloys: the case of Al- and Mn-doped ferritic steels. *Acta Mater.*, (169):284–300, 2019.

[7] R. Besson. Cluster variation method for investigation of multi-principal-element metallic alloys. *J. Alloys Comp.*, (952):170067, 2023.

[8] R. Besson. Point defects in multicomponent ordered alloys: Methodological issues and working equations. *Acta Mater.*, (58):379–385, 2010.

[9] J. Kwon, L. Thuinet, M.-N. Avettand-Fènoël, A. Legris, and R. Besson. Point defects and formation driving forces of complex metallic alloys: Atomic-scale study of Al_4Cu_9. *Intermetallics*, (46):250, 2014.

[10] L. Shao, T.-T. Shi, J. Zheng, H.-C. Wang, X.-Z. Pan, and B.-Y. Tang. First-principles study of point defects in C14 $MgZn_2$ Laves phase. *J. Alloys Comp.*, (654):475, 2016.

[11] R. Besson. Understanding phase equilibria in high-entropy alloys: II. Atomic-scale study of incorporation of metallic elements in Cr carbides – Application to equilibrium with AlCrFeMnMo. *J. Alloys Comp.*, (874):159959, 2021.

[12] R. Besson and L. Favergeon. Understanding the mechanisms of CaO carbonation: Role of point defects in $CaCO_3$ by atomic-scale simulations. *J. Phys. Chem. C*, (118):22583, 2014.

[13] E. Johansson, A. Ektarawong, J. Rosen, and B. Alling. Theoretical investigation of mixing and clustering thermodynamics of $Ti_{1-x}Al_xB_2$ alloys with potential for age-hardening. *J. Appl. Phys.*, (128):235101(1–12), 2020.

[14] E. Johansson, F. Eriksson, A. Ektarawong, J. Rosen, and B. Alling. Coupling of lattice dynamics and configurational disorder in metal deficient $Al_{1-\delta}B_2$ from first-principles. *J. Appl. Phys.*, (130):015110(1–14), 2021.

[15] Y. Han, Y. Dai, D. Shu, J. Wang, and B. Sun. First-principles calculations on the stability of Al|TiB_2 interface. *Appl. Phys. Letters*, (89):144107, 2006.

[16] C. Deng, B. Xu, P. Wu, and Q. Li. Stability of the Al|TiB_2 interface and doping effects of Mg/Si. *Appl. Surf. Sci.*, (42):639–645, 2017.

[17] Y. Ma, G. Ji, Z. Chen, A. Addad, and V. Ji. On the study of a TiB_2-nanoparticle-reinforced 7075Al composite with high tensile strength and unprecedented ductility. *Mater. Sci. Forum*, (941):1933–1938, 2019.

[18] Y. Ma, A. Addad, G. Ji, M. X. Zhang, W. Lefebvre, Z. Chen, and V. Ji. Atomic-scale investigation of the interface precipitation in a TiB_2-nanoparticles-reinforced Al–Zn–Mg–Cu matrix composite. *Acta Mater.*, (185):287–299, 2020.

[19] R. Besson, S. Macaluso, and L. Thuinet. Critical issues on coherent interface energy calculations revisited: The case of Al/TiB_2. *Surf. Interfaces*, (33):102272, 2022.

[20] X. Ma, C. Li, Z. Du, and W. Zhang. Thermodynamic assessment of the Ti–B system. *J. Alloys Comp.*, (370):149–158, 2004.

[21] V. T. Witusiewicz, A. A. Bondar, U. Hecht, S. Rexa, and T. Y. Velikanova. The Al–B–Nb–Ti system I. Re-assessment of the constituent binary systems B–Nb and B–Ti on the basis of new experimental data. *J. Alloys Comp.*, (448):185–194, 2008.

[22] V. T. Witusiewicz, A. Bondar, U. Hecht, J. Zollinger, L. V. Artyukh, and T. Y. Velikanova. The Al-B-Nb-Ti system: V. Thermodynamic description of the ternary system Al-B-Ti. *J. Alloys Comp.*, (474):86–104, 2009.

[23] B. Sundman, S. Jansson, and J. O. Anderson. The Thermo-Calc databank system. *Calphad*, (9):153–190, 1985.

[24] G. Kresse and J. Hafner. Ab initio molecular dynamics for liquid metals. *Phys. Rev. B*, (47):558–561, 1993.

[25] G. Kresse and D. Joubert. From ultrasoft pseudopotentials to the projector augmented-wave method. *Phys. Rev. B*, (5):1758–1775, 1999.

[26] J.P. Perdew, K. Burke, and M. Ernzerhof. Generalized gradient approximation made simple. *Phys. Rev. Lett.*, (77):3865–3868, 1996.

[27] J.P. Perdew, K. Burke, and M. Ernzerhof. Generalized gradient approximation made simple. *Phys. Rev. Lett.*, (78):1396–1396, 1997.

[28] P. E. Blöchl. Projector augmented-wave method. *Phys. Rev. B*, (50):17953–17979, 1994.

[29] M. Methfessel and A. Paxton. High-precision sampling for Brillouin-zone integration in metals. *Phys. Rev. B*, (40):3616–3621, 1989.

[30] Z.-K. Liu. Quantitative predictive theories through integrating quantum, statistical, equilibrium, and nonequilibrium thermodynamics. *J. Phys.: Condens. Matter*, (36):343003, 2024.

[31] R. Liu, X. Yin, K. Feng, and R. Xu. First-principles calculations on Mg|TiB_2 interfaces. *Comput. Mater. Sci.*, (149):373–378, 2018.

[32] B. Meyer and M. Fähnle. Atomic defects in the ordered compound B2-NiAl: a combination of ab initio electron theory and statistical mechanics. *Phys. Rev. B*, (59):6072–6082, 1999.

[33] R. Besson, A. Legris, and J. Morillo. Influence of complex point defects in ordered alloys: An ab initio study of B2 FeAl-B. *Phys. Rev. B*, (74):094103, 2006.

[34] C. Thenot, R. Besson, P. Sallot, J.-P. Monchoux, and D. Connétable. Interactions of oxygen with intrinsic defects in $L1_0$ γ-TiAl in presence of substitutional solutes: Influence on diffusion kinetics. *Comput. Mat. Sci.*, (201):110933, 2022.

[35] Z. Fan, Y. Wang, Y. Zhang, T. Qin, X. R. Zhou, G. E. Thompson, T. Pennycook, and T. Hashimoto. Grain refining mechanism in the Al/Al-Ti-B system. *Acta Mater.*, (84):292–304, 2015.

[36] J. Fjellstedt, A. E. W. Jarfors, and L. Svendsen. Experimental analysis of the intermediary phases AlB_2, AlB_{12} and TiB_2 in the Al–B and Al–Ti–B systems. *Journal Alloys Comp.*, (283):192–197, 1999.

[37] D. Tingaud and R. Besson. Point defects and diffusion in ordered alloys: An ab initio study of the effect of vibrations. *Intermetallics*, (45):38, 2014.

[38] D. Tingaud and R. Besson. Point defect phonons in intermetallics: $NiAl_3$ by atomic-scale simulation. *Phys. Stat. Sol. C*, (6):2008–2011, 2009.

[39] D. Gryaznov, E. Blokhin, A. Sorokine, E. A Kotomin, R. A. Evarestov, A. Bussmann-Holder, and J. Maier. A comparative ab initio thermodynamic study of oxygen vacancies in ZnO and $SrTiO_3$: Emphasis on phonon contribution. *J. Phys. Chem. C*, (117):13776–13784, 2013.

[40] R. Besson and R. Candela. Ab initio thermodynamics of fcc H-Zr and formation of hydrides. *Comput. Mater. Sci.*, (114):254, 2016.

[41] A. V. Bakulin and S. E. Kulkova. Effect of impurities on the formation energy of point defects in the gamma-TiAl alloy. *J. Experim. Theoret. Phys.*, (127):1046–1058, 2018.

[42] V. Vaithyanathan, C. Wolverton, and L. Q. Chen. Multiscale modeling of precipitate microstructure evolution. *Phys. Rev. Lett.*, (88):125503, 2002.

[43] V. Vaithyanathan, C. Wolverton, and L. Q. Chen. Multiscale modeling of θ' precipitation in Al-Cu binary alloys. *Acta Mater.*, (52):2973–2987, 2004.

[44] S. Y. Hu, M. I. Baskes, M. Stan, and L. Q. Chen. Atomistic calculations of interfacial energies, nucleus shape and size of precipitates in Al-Cu alloys. *Acta Mater.*, (54):4699–4707, 2006.

[45] Y. Mishin, M. Asta, and J. Li. Atomistic modeling of interfaces and their impact on microstructure and properties. *Acta Mater.*, (58):1117–1151, 2010.

[46] X. J. Ye, C. S. Liu, W. Zhong, and Y. W. Du. Precipitate size dependence of Ni/Ni_3Al interface energy. *Phys. Lett. A*, (379):37–40, 2015.

[47] L. Thuinet and R. Besson. Ab initio study of competitive hydride formation in zirconium alloys. *Intermetallics*, (20):24, 2012.

[48] M.-A. Louchez, R. Besson, L. Thuinet, and A. Legris. Interfacial properties of hydrides in alpha-Zr: a theoretical study. *J. Phys.: Condens. Matter*, (29):415001, 2017.

[49] Z.-K. Liu. First-principles calculations and CALPHAD modeling of thermodynamics. *J. Phase Equilib. Diff.*, (30):517–534, 2009.

[50] Z.-K. Liu. Thermodynamics and its prediction and CALPHAD modeling: Review, state of the art, and perspectives. *Calphad*, (82):102580, 2023.

[51] OPTIMADE, Open Databases Integration for Materials Design consortium. *https://www.optimade.org*.

[52] MPDD-eXchange, solution for getting material properties with ML models. *http://mat-x.org*.

[53] Z.-K. Liu. Computational thermodynamics and its applications. *Acta Mater.*, (200):745–792, 2020.

[54] MAterials Properties Prediction (MAPP). *https://faculty.engineering.asu.edu/hong/materials-properties-prediction-mapp/*.